Ravine alluvial fans as records of landscape change in the Le Sueur River Basin, southern Minnesota

A Thesis
SUBMITTED TO THE FACULTY OF
UNIVERSITY OF MINNESOTA
BY

Ian Treat

IN PARTIAL FULFILLMENT OF THE REQUIREMENTS
FOR THE DEGREE OF
MASTER OF SCIENCE

Dr. Karen Gran, Advisor

October, 2017

Acknowledgements

This project was funded in part by the Minnesota Department of Agriculture, the Clean Water Land and Legacy Amendment, and the National Science Foundation (EAR – 1209402). Comments from Karen Gran and my committee, John Swenson and Tongxin Zhu, were invaluable to this project. Field guidance from Phil Larson (Minnesota State University), sample technique development from David Grimley (Illinois State Geological Survey), and electron microscope training from Tsutomu “Shimo” Shimotori (UMD) are greatly appreciated. Most of all, this project would not have accomplished as much without the dedication from my field and lab assistants, Evan Lahr and Austin Cavallin. Thanks to my friends and family for their continual support throughout this project.

Abstract

Ravine alluvial fans in the Le Sueur River Basin (LSRB) of south-central Minnesota record post-glacial Holocene changes and modern anthropogenic disturbances to land cover and hydrology in high-latitude watersheds. Seventy meters of base-level drop at the end of the last glaciation initiated millennia of incision that continues on the LSRB today. Onto this template of on-going incision, Euro-American land clearing and drainage of previously stable upland prairie and wetlands in the mid-1800s further increased erosion rates in the basin. Ravines, first-order channels that link low-gradient uplands with the deeply-incised channel network, experienced changes in erosion rates over time from both impacts, with the erosional history preserved in alluvial fans at the mouths of ravines where they terminate on fluvial terraces (Figure 1).

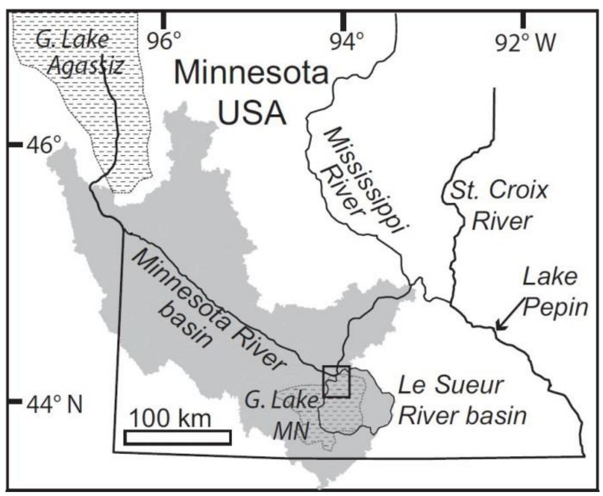

Figure 1. The Le Sueur River Basin within the Minnesota River Basin. Glacial Lake Agassiz to the northwest was responsible for rapid base-level change on the Le Sueur River (Gran et al., 2013).

Establishing a post-settlement chronology is difficult in the highly erosive knickzone of the Le Sueur. We take advantage of six fan deposits spread throughout the LSRB to determine the fluvial response of upland agricultural land conversion on steep first-order drainages. Ravines respond quickly to sediment and hydrology fluxes in the basin that are

reflected in their alluvial fans as packages of post-settlement alluvium (PSA) and incision through fan surfaces. Bulk soil samples collected at 10-, 20-, 40-, 100-, and 200-centimeter depths on the selected fans as well as samples from the incised channel were analyzed for fly ash, spherical silt-sized grains that are a byproduct of coal combustion. The presence of fly ash as an in-situ stratigraphic marker at depth was used to calculate conservative post-settlement deposition rates of 0.93 and 1.67 cm/yr using observation techniques from high-powered transmitted and reflected light microscopes as well as scanning electron microscopy, respectively. These rates are a three-fold increase over generous Holocene deposition rates of 0.27 cm/yr. Incision through fan surfaces also marks post-settlement changes. Trenching and tile drainage on the uplands allowed for greater transport of water down ravines and onto fans. These results confirm land use change triggered an increase in upstream erosion and fan deposition followed by incision on short time scales.

Table of Contents

List of Tables

List of Figures

Introduction

Ravines are large, geomorphically-sensitive gullies that connect areas of higher elevation to the river channel (Poesen et al., 2003). Climate, vegetation, and land use change determine the capacity and efficiency of ravine erosion and sediment production (Poesen et al., 1996; Gábris et al., 2003; Rey, 2003; Hooke, 2006; Hooke and Sandercock, 2012). Driving forces (climate and slope) and resisting forces (vegetation and soil cohesion) govern a ravine's evolution. Changes in one parameter often affect other variables in this balance. For instance, persistent droughts may reduce plant density and population resulting in soil degradation and fluvial transport.

Climate is the most effective control on ravine formation in terms of the delivery of precipitation and its effect on vegetation. Ravine erosion rates in humid climates are more constant because of seasonal uniformity in broad sweeping warm or cold fronts (Ries and Marzolff, 2003; Novotny and Stefan, 2007). In Mediterranean and semi-arid climates precipitation tends to be more localized and intense (Bull et al., 1999; Esteves and Lapetite, 2003). The highest erosion rates are found here because there is enough precipitation for soil development but not enough to sustain dense vegetation.

Ravines behave differently in more arid climates (Nogueras et al., 2000; Martínez-Casasnovas, 2003; Vanacker et al., 2003; Vandekerckhove et al., 2003;) versus temperate climates (Thomas et al., 1986; Burkard and Kostaschuk, 1995; Poesen et al., 1996; White, 1996; Gábris et al., 2003; Rey, 2003; Strunk, 2003; Nagasaka et al., 2005; Dotterweich, 2008). Arid and semi-arid climates receive less precipitation because they are not as moderated as temperate or tropical climates; therefore, ravines in arid environments behave flashier than temperate streams and can be highly erosive. In addition, low precipitation leads to less vegetation. For example, throughout much of Spain, it was found that ravines contribute as much as 80 percent of the sediment to the river's budget (Poesen et al., 1996; Martínez-Casasnovas, 2003), and the rate that gullies retreat in semi-arid and arid environments is faster than temperate climates (Vandekerckhove et al., 2003; Poesen et al., 2003).

Vegetation is paramount to a soil's stability. When land is repurposed and vegetation is changed or removed, soil is exposed to the elements and becomes easier to transport. Grass, trees, and shrubs anchor soil so that it does not become mobile in runoff. Plants are responsible for retaining the slope of the ravine, and they can be used to control soil loss (Hooke and Sandercock, 2012). The denser the vegetation, the more energy overland flows must have to remove sediment and transport it (Gyssels et al., 2005). Vegetation density also affects spatial variability for erosion (Rey, 2003; Hooke, 2007). Hypothetically, a ravine may have 75 percent vegetation cover, but if vegetation is not in the active region where water flows in the channel, erosion rates and ravine incision might remain the same or only slightly decrease (Oostwoud Wijdenes et al., 2000). The presence of vegetation at the tips of ravines or in the base of them also identifies if gullies are active or not. The most stable gullies are those that have well-developed ground cover at the channel base (Nogueras et al., 2000). Even steep-sloped bank gullies with moderate cover may be considered inactive compared to a more gently-sloping gully with little or no vegetation.

Repurposing presently stable land into agricultural land and forest clearing can disturb the stability of the system and cause soil loss in agrarian regions (Thomas et al., 1986; Burkard and Kostaschuk, 1995; Poesen et al., 1996; Gábris et al., 2003; Hooke, 2006). This is most common in situations where native grassland, prairie, or forest was converted to row crop agriculture. Conversion from shrub land to plantations or other bare land often induces erosion (Nogueras et al., 2000). In Mediterranean regions, land use change by vegetation clearing was identified as the major cause of sediment removal (Hooke, 2006). Studies conducted on gully erosion in agricultural lands draw the same conclusion: land use change to row-crop agriculture increases gully contributions in the watershed sediment budget (White, 1996; Oostwoud Wijdenes et al., 2000; Gábris et al., 2003).

Ravines can be a significant source of sediment, but the role they play in sediment loading at a basin scale varies greatly depending on local conditions (DeRose et al., 1998; Martínez-Casasnovas, 2003). Land use change in different climates of the world affects ravine evolution uniquely. Given ravine sensitivity to elements like climate, vegetation, and land use, how do ravines respond to anthropogenic changes like land use change and water delivery to the system in a humid, temperate climate? How are depositional records preserved in these rapidly eroding systems and how do we go about finding them? To address these questions, I worked in the Maple, Cobb, and Le Sueur Rivers of the Le Sueur River Basin (LSRB) in south-central Minnesota because of its natural and modified geomorphic instability. Euro-American settlers overturned the prairie grasses in the LSRB, and replaced them with predominantly corn-soy rotation crops (Musser et al., 2009). Changes in drainage followed the introduction of widespread agriculture, leading to a complex series of impacts on the ravines and their upstream watersheds. We cored alluvial fans at the bases of six ravines to investigate how anthropogenic driving forces impacted the ravines. Because of the complexity of ravine response to sediment and water delivery, we looked for records of both deposition and incision on alluvial fans.

Background

Ravines in the LSRB exist because of a 70-meter base level drop in the Minnesota River channel from the drainage of glacial Lake Agassiz (Gran et al., 2009). Incision propagated upstream as a knickpoint through tills and weak Paleozoic bedrock, creating bluffs that line valley walls and ravines that connect the flat uplands with the deeply-incised channel. Mainstem river incision induced geomorphic instability and created erosional hotspots further destabilized by anthropogenic activity. Of the 106 ravines in the basin, most are ephemeral, but some of the largest ones flow year round.

Ravines behave differently as the river shifts position in the valley. Ravines that remain directly connected to the channel have been able to keep up with base level fall or have reconnected with the channel after previously being cut off. Many of the larger ravines that connect to the mainstem channel are found below the knickzone where the channel has equilibrated to base level fall and had time to reconnect with the mainstem rivers. Ravines that are cut off from the main channel by meander migration and incision terminate on terraces where these ravines are able to construct alluvial fans.

Changing land use affects sediment erosion and storage in a basin (Belmont et al., 2011; Gran et al., 2013). Western settlers extensively modified the land in the LSRB. They plowed the fertile upland prairies for diverse agricultural use while the ravines were cleared for timber—something the prairies are largely devoid of—for construction. This broke up soil structure, mobilizing sediment in the basin. Because the upland topography is flat, water drains slowly from the prairie. Thus, drainage ditches were dug, and later, drainage tiles were installed beneath the fields to remove standing water. Although this was beneficial for farmers, this impacts ravine response to precipitation events.

The meandering and incising channels of the incised zone lack storage due to limited floodplains and in-channel storage. However, alluvial fans retain a thorough depositional archive on terraces with basal ages that date back as far as the inception of the terraces. Overland flow transported sediment through ravines and deposited them on alluvial fans, leading to an archive that potentially recorded the impacts of changes in land use and hydrology. If the basal ages do correlate with the ages of terraces, then sediment deposits should record pre- and post-settlement changes.

There are two end member hypotheses on the development of these alluvial fans. The first is that the ravines and fans are simply a part of base-level adjustment cycle, and that fan deposition is an ongoing process that began when the ravine was cut off from the mainstem channel—a process that has been occurring throughout the Holocene as the valley has been excavated. In this case basal fan ages should match terrace ages because the time of terrace formation is the point at which the channel is no longer connected to the river and sediment starts building a fan; deposition rates would remain roughly constant over time. The second possibility is that these alluvial fans are primarily composed of rapidly aggrading sediment called post-settlement alluvium (PSA). PSA contains physical objects like coal, metal fragments, and other waste (Phillip Larson, personal communication) as well as microscopic markers to be discussed later. If this hypothesis were true, alluvial fans would have deposited more rapidly because of upland land use changes, and most of the sediment in fans would be PSA.

The arrival of Euro-American settlers in the mid-1800s brought significant land use change to the basin. During the post-settlement transition period, Lake Pepin, downstream from the LSRB on the mainstem Mississippi River, experienced a ten-fold increase in deposition during settlement with most of that sediment sourced in the Minnesota River Basin (Kelley et al., 2006; Engstrom et al., 2009; Belmont et al., 2011). The Le Sueur River is the source for as much as 30 percent of the sediment in the Minnesota River, which, in turn, is the source for 80 to 90 percent of the sediment in Lake Pepin in the upper Mississippi River.

Changes in sediment fluxes were not the only post-settlement effects on ravines. Western settlement also changed how water drained from the fields and through ravines. With increasing intensity during the 19th and 20th centuries, ditches and tile drains were installed to remove standing water from fields, and many of these drains now terminate at ravine tips. The increased water in the ravine-alluvial fan system caused ravines to incise deeper and through their alluvial fans to meet this change, yet detailed response to changes in hydrology is largely unknown. Some landowners also ditched the lower ends of ravines and reconnected them with the main channel. This allowed ravines that once terminated on terraces to experience the base level change that continued when the rivers incised further.

This research explores alluvial fans as archives for post-settlement change in the LSRB, specifically how land clearing and subsequent changes in hydrology affected erosion rates in ravines and deposition rates on fans. Changes in hydrology may not reveal themselves as lower or higher deposition rates but instead as incision. This research thus focuses on techniques for identifying PSA on ravine alluvial fans, identifying stratigraphic markers in fan sediments, and making observations of incision through alluvial fans.

There are several techniques utilized to find settlement horizons in Holocene settings. Late Holocene material is commonly dated using carbon-rich material to constrain ages of material to build chronologies (Evans et al., 2004; Bogemans et al., 2012). Another method gaining popularity, especially in former glaciated terranes, is pollen identification (Lewis and Birnie, 2001; Willard et al., 2003) where *Ambrosia* (ragweed), specifically, is used as a marker of soil disturbance (Craine and McLauchlan, 2004). It is used in lacustrine environments where anoxic conditions preserve pollen taxa. In oxic conditions, *Ambrosia* does not preserve well and decomposes quickly, and it was discarded as a technique for PSA in ravines (Campbell, 1999; Li et al., 2005; Twiddle and Bunting, 2010).

Another method gaining popularity to document post-settlement conditions is fly ash as a byproduct of coal combustion (Locke and Bertine, 1986; Jones and Olson, 1990; Kapicka et al., 1999; Grimley et al., 2004; and Grimley and Arruda, 2007). Its magnetite composition makes it easy for extraction in sediment, and its spherical morphology make it easy to identify under visible and scanning electron microscopes. Fly ash sources directly from anthropogenic processes, and it is a relatively inexpensive stratigraphic indicator in post-settlement alluvium (Grimley et al., 2017). Here I use fly ash as a marker of PSA to compare pre- and post-settlement depositional rates on ravine fans deposited on stream terraces throughout the LSRB.

Methods

Site Selection and Lidar Analysis

Lidar analyses were used to determine field sampling sites and better observe interactions between the ravine-fan system and the main channel. To get an accurate basin-wide survey of PSA, variance among many parameters was ideal. Selection criteria included position of ravines and their alluvial fans on the main stem channel with varying distances upstream as well as the size, evolutionary stage, terrace elevation, and geographical location of the fan. Fans needed to have easy access to transport sampling equipment. Six sites were selected that met all the criteria set for field sampling (pending landowner permission): three on the Le Sueur, two on the Maple, and one on the Big Cobb (Figure 2).

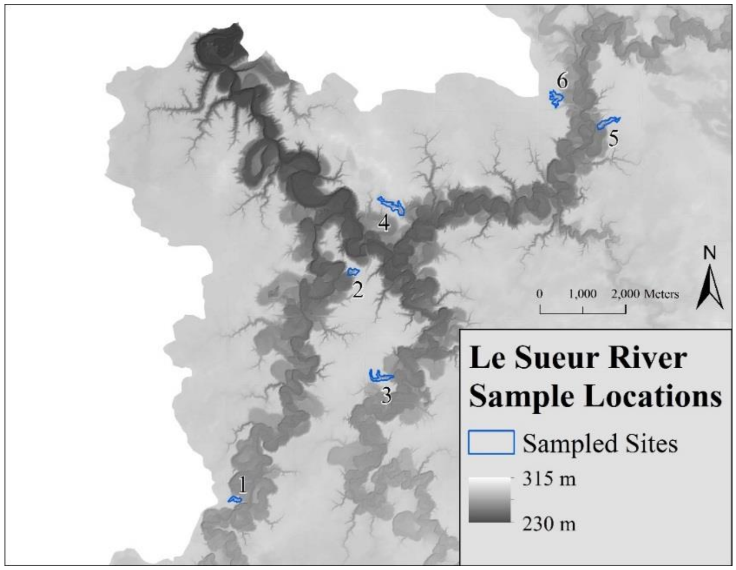

Figure 2. Location of the six sample sites within the incised zone of the LSRB. There are two sites on the Maple River, one on the Cobb River, and three on the Le Sueur River. 1) Mel, 2) Magdalena, 3) Catalina, 4) Leigh, 5) Lola, 6) Loren.

Geomorphic processes in the ravines and their fans reflect the changing hydrology and sediment fluxes in the uplands and the disconnection and reconnection to the mainstem river. Using one-meter resolution lidar data, I classified ravines based on their interaction with the modern channel. I set up a system to classify where in the hypothesized evolutionary trajectory each ravine system lay concerning its hydraulic relationship with each of the main channels (Table 1). I did this for all 106 ravines in the LSRB to assist with site selection to find six sites in the knickzone. I wanted to sample five sites that built alluvial fans, but were undergoing incision, and I wanted to sample one fan that built an alluvial fan without incision. I targeted five fans that were “0” and “2” because of their ability to archive sediment and hydrology changes, and one fan that was just “2.” Other fans classified as “1” terminated on a terrace with or without a fan. In addition to the ravine classification system, I developed a series of hypotheses for potential ravine alluvial fan behavior based off the balance of water versus sediment fluxes in the system resulting from changing land use (Table 2) (Figure 3a-f).

Table 1. Ravine classification system.

0	Ravine terminating in the main channel
1	Ravine terminating on terrace
2	Ravine building an alluvial fan

Table 2. Alluvial fan evolutionary hypotheses.

H0	Continuous alluvium deposition
H1	Ravine with a PSA package
H2	Incision without PSA
H3	Incision with PSA

Unlike the ravine classifications, which were determined solely based on lidar before fieldwork, the alluvial fan response required fieldwork to determine the extent of PSA deposition on the fan surface. H0 represents alluvial fans that have undergone continuous, relatively uniform, background deposition and incision throughout the Holocene. H1 refers to a fan that shows increased deposition rates, seen as thick packages of PSA on top of older Holocene sediments. H2 is a fan where land use changes led to increased incision rates, so no or little PSA accumulated on the fan surface, yet deeply incised channels would cut through the surface as a response to changing hydrology. Finally, H3 is a fan that deposited a PSA package on top of Holocene alluvium then was dissected by an incising channel indicating impacts first by land clearing then by increased flows. On a surface, this is a thick PSA package on top of Holocene sediment and incision cutting through the fan. Alluvial fans with dissecting channels were prime candidates for sampling because of visual exposures and sampling access. Fieldwork coupled with laboratory analyses determined if PSA deposited on top of the fans and its extent.

Field Observations and Extraction

Fieldwork in the LSRB consisted of recording detailed field observations like slope of the ravine, depth of incision, sediment color, grain size, and the presence of organic material.

On each of the alluvial fans, I surveyed two to three radial transects down the fan from the apex to the distal fringes of the fan (depending on its size). Then, I hand augered into the fan surface using a two-meter long hand auger with a four-inch diameter drill bit referencing each auger location with a handheld GPS unit for further referencing in GIS. At 10-, 20-, 40-, 100-, and 200-centimeters, I measured the depth of the hole and bagged a sample of sediment in a quart-sized ziplock bag at each location. All sites had samples collected between 10 cm and 200 cm down from the surface. While I planned to collect samples down to 200 cm at all sites, I made some momentary decisions in the field because of unforeseen difficulties in sampling. The sediment was stored for grain size analysis and future investigation of post-settlement alluvium markers including fly ash. I used visual reference cards from the Rite in the Rain Geological Field Notebook to determine grain size. Grain size correlates to the energy needed to transport material onto the fan surface. This aided in interpreting depositional history.

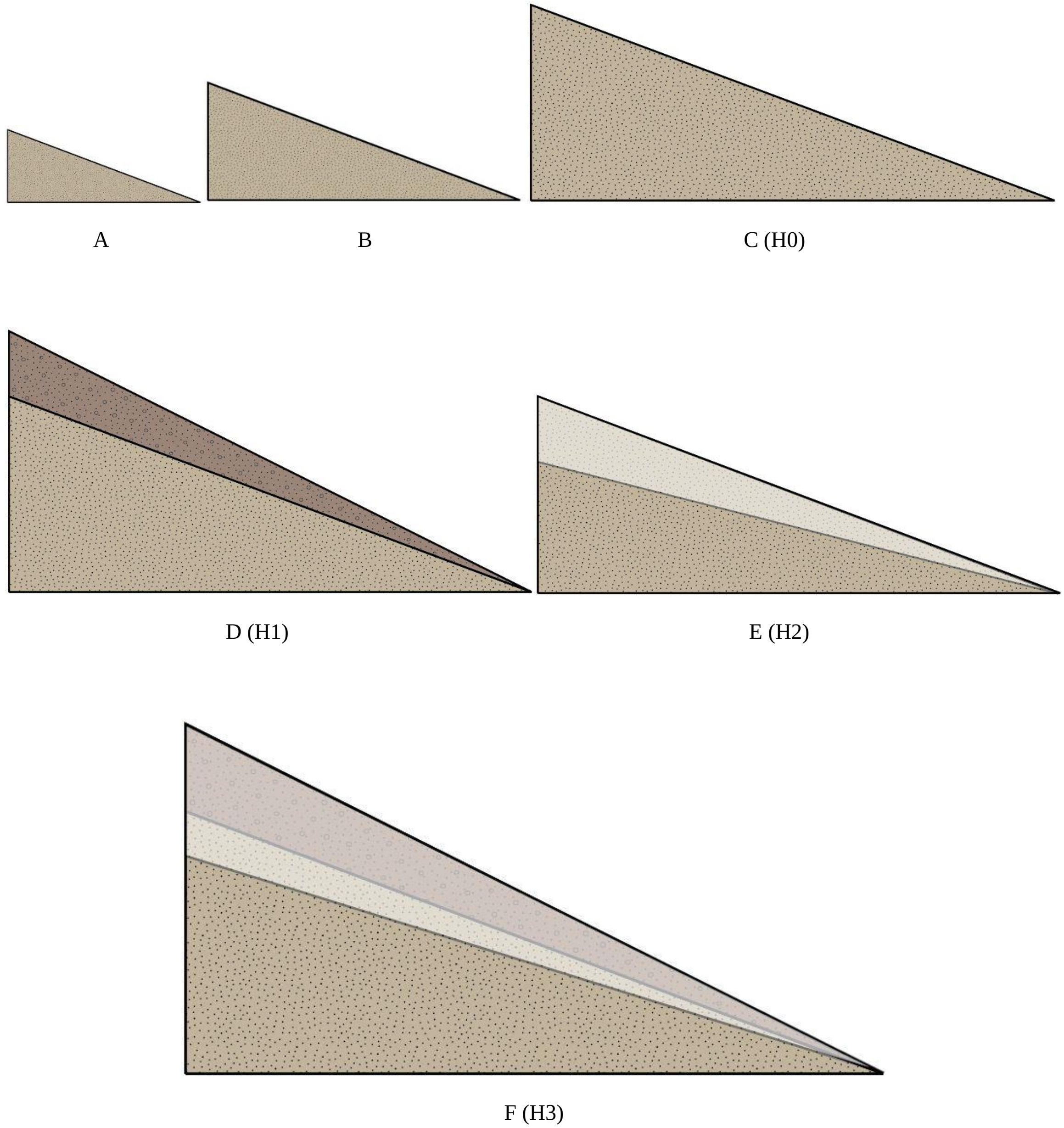

Figure 3a-f. A and B show the development of Holocene alluvium since the abandonment of the terrace it deposits on. C-F are the four evolutionary fan hypotheses in the LSRB highlighted in Table 2. C is a fan that only exhibits continuous Holocene deposition. D is an alluvial fan that recorded greater sediment inputs by depositing a PSA package on top of Holocene alluvium. E is a fan that experienced incision as a result of changing hydrology. F experienced PSA deposition first recorded PSA deposition then experienced incision.

Fly Ash Method Development

Grimley et al. (2017) quantify fly ash by a randomized 100-grain point count of the magnetic grains in a sample. Their study focused on fly ash presence in floodplain material. Floodplains preserve fly ash better than ravine-sourced alluvium as overbank flows deposit fine sediment in static reaches. One of the challenges to modifying Grimley's technique was transferring the methods from one geologic setting to another because no literature exists where fly ash was used as a proxy for Western settlement on alluvial fan surfaces.

The methodology for fly ash extraction used here is based off the work from Grimley et al. (2017) with some of the finer details modified (Appendix 1). Data extraction began upon return to the lab with more than 200 sediment bags of loose alluvium. Samples were sieved, extracted from solution, and analyzed using microscopy. Because fly ash is silt-sized, I sieved 20 grams of dried alluvium using a 125-micron sieve. The separated material was placed in a 400-mL beaker and 250-mL of de-ionized water was added along with 10-mL of sodium-hexametaphosphate used for particle disaggregation. Fly ash is composed of magnetite and is magnetically susceptible. I ran the solution for two mixing cycles with a magnetic stirrer (the first for five minutes and the second for two minutes) to attract as much magnetically-susceptible material as possible. Occasionally, enough magnetic material agglomerated after the first magnetic mixing to isolate it for drying and visual analysis. After each mixing cycle, I rinsed the magnetic stirrer with de-ionized water into a separate 100-mL beaker that stored the magnetic fraction in solution. In an oven at 50-degrees Celsius, I evaporated off the solution leaving the dried magnetic fraction. That was isolated from the 100-mL beaker into 1-in by 1-in by 0.5-in clear, plastic cubes for storage and microscope analysis.

Standard technique involves 100-grain point counts under a visual light microscope coupled with scanning electron microscope (SEM) analysis for more magnified observation and elemental analysis using energy dispersive spectroscopy (EDS) (Appendix 6). This was crucial in determining fly ash because there are other grains having similar morphology to fly ash but with different composition. This technique retains the fly ash extraction and analysis process, but it has its own set of challenges. Ravine alluvium is coarser and deposits under different conditions than floodplain material. Preliminary results when adapting the technique indicated that fly ash densities were much lower than in Illinois, so I was unable to conduct a standard 100-grain point count under a visual light microscope. To improve resolution in the samples, I devised three observational techniques that would draw from different parts of the data set to form conclusions on fly ash. The first survey was a simple presence-absence visual pass for every sample under a Zeiss reflected and transmitted light microscope at 250-x magnification (Appendix 2). For the second, I selected one bore hole location from each fan for a high-resolution survey. I made SEM mounts on a JEOL JSM-6490LV for the top and bottom sample of the sediment column. To reduce the raw magnetic fraction size, I 3D-printed a sediment splitter to subdivide the magnetic fraction into six equal parts. I placed the split magnetic fraction on an SEM mount, and I counted every fly ash grain visible (Appendix 3). After understanding the behavior and placement of fly ash within the magnetic fraction, I modified my visual investigation techniques from the presence-absence survey to look more closely at fly ash under a visual light microscope for the final survey. I counted each fly ash grain from every sampling interval at one bore hole to compile a medium-resolution survey (Appendix 4). This medium-resolution survey would highlight any patterns that might otherwise go unnoticed in the high-resolution SEM survey but more quantifiable than a low-resolution presence-absence survey.

Deposition Rate Calculation

Terrace ages were calculated using results from a one-dimensional numerical model from Gran et al. (2013). Distance upstream and terrace height above the main channel at ten-year intervals from 13.5 ka to the present were outputs for the model. It gives a hypothetical floodplain elevation with a distance upstream at different points in time, thus allowing me to back-calculate the estimated age of the surface. The main channels abandoned terraces through incision. We hypothesize that alluvial fans began depositing on terraces immediately after abandonment. This gives a basal fan age. The PSA depth divided by the age of the terrace calculates a Holocene-averaged deposition rate. Three radiocarbon dates were collected during early site selection reconnaissance (Table 3), but suffered from problems related to remobilization and deposition of older materials, as well as a lack of dateable material in many cores. Because I lacked abundant, reliable dateable material, I also abandoned further radiocarbon dating as a method.

Table 3. Alluvial fan radiocarbon dates.

Location	**Depth (cm)**	**Age (years BP)**	**Terrace age (years BP)**
Mel 8	125	300 ± 30	3360
Leigh 2	180	3710 ± 30	4020
Leigh 7	440	16520 ± 60	4020

Fly ash at depths marked horizons of change from land clearing events on the uplands and in the ravines. Assuming a period of deposition, we calculated rates of post-settlement deposition based on the depth of fly ash in stratigraphy. Repeat lidar was also used to estimate modern short-term erosion rates with lidar flown in 2005 and 2012 (Schaffrath et al., 2012). I isolated the regions within the ravines and calculated the net erosion/deposition from each feature.

Fly Ash Background

Fly ash was used as a marker of post-settlement deposition following the methodology of Grimley et al., (2017). The most likely source for fly ash for this study area is the city of Mankato and the surrounding hub and spoke network of abandoned railroads (Figure 4). Mankato has long been a hub for railroads in the Midwest. The first railroad arrived in 1868, and rapid population growth from near 3,000 in 1868 to 10,599 in 1900 fueled its network expansion and service frequency (Blue Earth County Historical Society). All the steam locomotives were coal-burning, and dieselization did not occur until the 1950s. The Chicago, Milwaukee, & St. Paul Railroad traced north from Mapleton to Good Thunder and terminated in Mankato; it closed in the 1970s. There is no way to distinguish fly ash from steam locomotives versus coal-fired industry, but fly ash pollution was banned in the 1970s with the installation of scrubbers from the passing of the Clean Air Act.

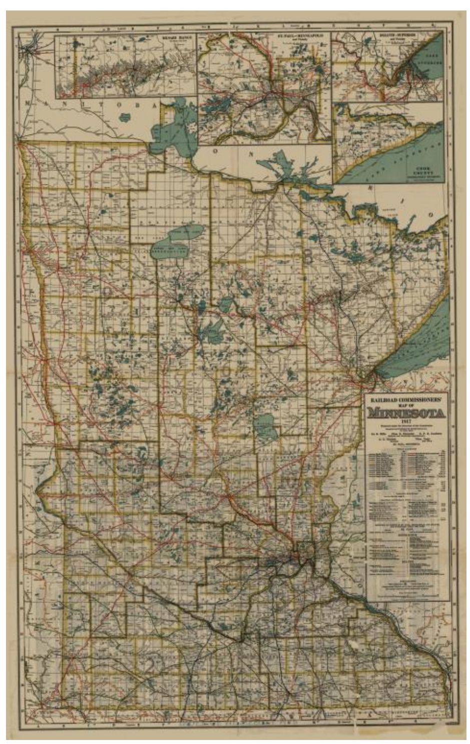

Figure 4. Map of historic railroads from 1917.

In Illinois, where this methodology was first developed, the dominant source of fly ash was coal power plants (Grimley et al., 2004; Grimley and Arruda, 2007; Grimley et al., 2017). In Mankato, coal-fired plants were constructed for industrial use, not large-scale power generation. A coal gas plant was constructed in 1883 for street lighting, and the Hubbard Mill was a large consumer of steam coal (a gradient between lignite and bituminous). Other agricultural processing facilities used coal. With these historic dates, I can estimate a period of fly ash deposition—1868 being the earliest with the arrival of steam locomotives, and 1970 being the latest with the passing of the Clean Air Act. This constraint aids me in calculating rates of PSA deposition in my results. However, a more realistic late age bracket ends fly ash production in the 1950s with the retiring of steam locomotives.

Results

Field Observations

All the land upstream of the incised ravines is in row-crop agriculture, but each sampled ravine has a unique geometry that reflects the erosional and depositional history. Below I describe each ravine in detail and then present the results from the stratigraphy and fly ash analyses (Table 4) (Figure 5) (Figure 6) (Figure 7a-f).

Mel

Mel is located within a highly erosive reach of the Maple River. The alluvial fan deposited on the boundary between two terraces with about one-meter elevation difference. The change in slope is clearly visible on the lidar DEM where the ravine alluvial fan channel changed to the lower terrace. The channel dissecting this fan cut down two meters, and alluvial deposits visibly line the incised walls (Figure 8). Small freshwater snails are in abundance within the alluvium. The residents on this property commented on the expansion and widening of the ravine in recent decades. They say more water flows through the ravine more often. There are two transects surveyed onto the fan surface with one point outside the transect paths. All were sampled for fly ash except for Mel 5 because it was too rocky. Mel 1 and Mel 8 were at the apex of the fan, but Mel 8 was collected from inside the incised channel.

Magdalena

The smallest of the sampled fans, Magdalena is also the only sampled ravine that does not have a channel dissecting it. It is perched on a low terrace near the confluence of the Maple and Le Sueur Rivers. Its alluvial fan is miniscule, yet it still yields fly ash. There is evidence for channelized flow down the centerline of the fan, but it was ephemeral and not flowing during the time in which sampling occurred. Magdalena has two transects emanating from its apex with each sample hand augered.

Catalina

The only site on the Cobb River, Catalina is a large ravine with eight meters of incision from the fan apex surface to the wide, incised channel. The terrace on which the fan deposited is truncated laterally from when the river eroded into it when it was at a lower level. The incised channel is very sandy, and, like Loren, it appears to be filling itself in. The owners had the county road commission grade the channel another direction because it was forming a new alluvial fan on an agricultural field on a lower terrace. The fan is also radial in shape and is vegetated by tall grass. There were two transects surveyed on Catalina each on either side of the incised channel.

Table 4. Ravine and alluvial fan metrics.

Name	River	Number of Samples	[2]Fan Apex Northing (m)	[2]Fan Apex Easting (m)	Distance Upstream from Le Sueur-Blue Earth Confluence(km)	Elevation (m asl)	Height above channel (m)	Ravine Area (m^2)	Ravine Volume (m^3)	Fan Area (m^2)	Fan Volume (m^3)	Incision into Fan Surface (m)
Mel	Maple	8	416323	4875376	16.0	282.7	10.3	21246	537517	22128	24252.9	0.33
Magdalena	Maple	7	418949	4880523	3.4	265.6	12.8	7992	106131	1581	8126.2	0
Catalina	Cobb	7	419793	4878237	8.2	281.5	12.9	53623	499889	16141	18499.98	0.78
Leigh	Le Sueur	7	420113	4882011	15.2	277.5	27.1	74441	358804	33459	41988.06	0.76
Lola	Le Sueur	10	424750	4884031	25.9	272.6	8.7	49788	721315	11058	17333.74	0.21
Loren	Le Sueur	6	423826	4884767	27.3	283.1	16.8	53333	403886	34940	*[1]	0.23

[1]Loren was not sampled on its alluvial fan. [2]Coordinates based off NAD83 UTM Zone 15N.

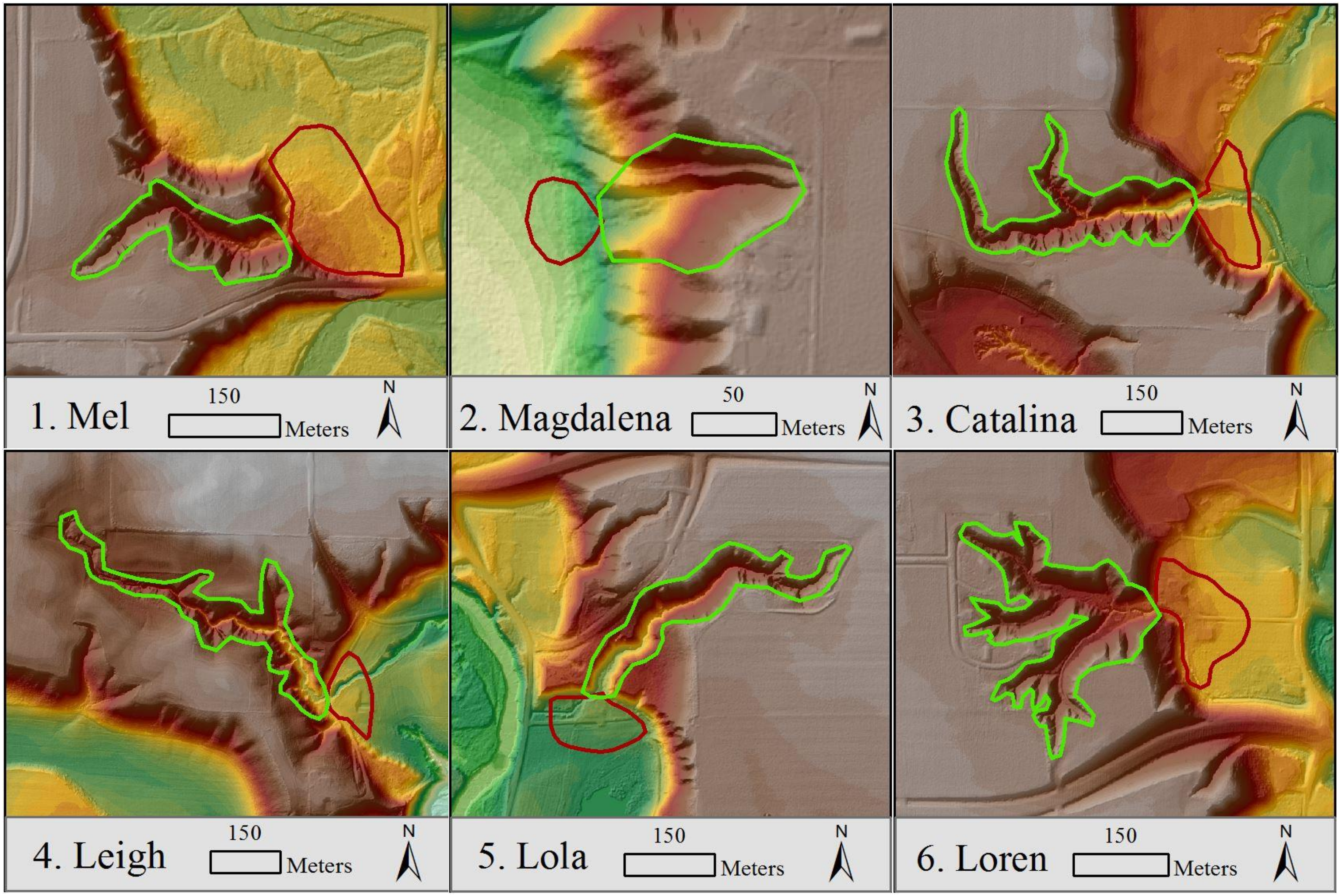

Figure 5. Close-up figures of the sample sites. Green polygons are ravines, and red polygons are alluvial fans.

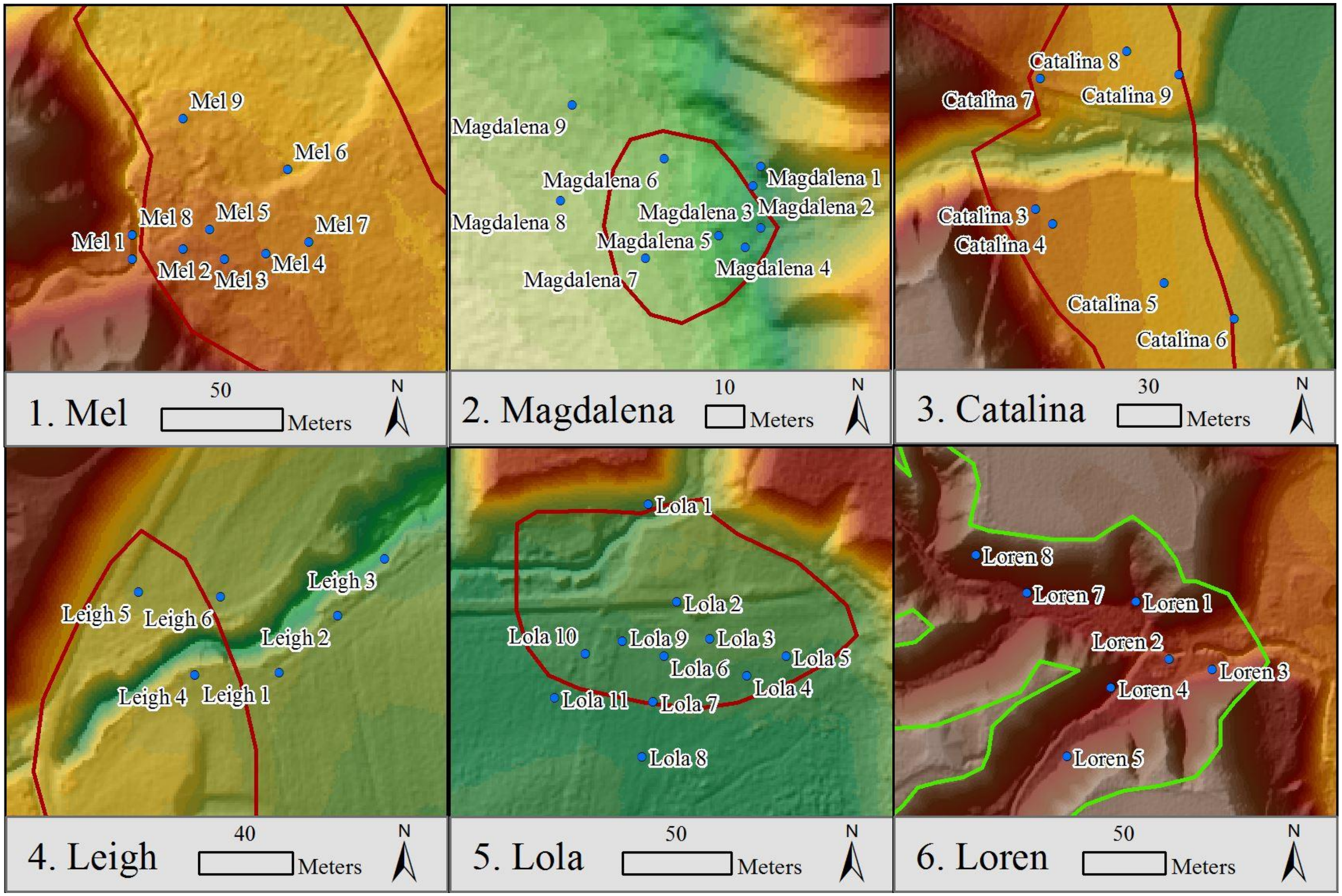

Figure 6. Map with sample locations on all sites.

Figure 8. Stratigraphy of the incised alluvial fan wall on Mel.

Leigh

Downstream from Loren and Lola, Leigh is perched on a high terrace on the right bank of the Le Sueur. It has the largest alluvial fan by surface area and volume and the most incision dissecting the fan. The landowner on Leigh has a driveway that crosses over the apex of the fan at the mouth of the ravine. The culvert under the road has fixed the knickpoint with seven meters of incision in the fan and backfill deposition forming in the ravine filled with sediment and forest debris upstream of the driveway. Much of the stratigraphy is sandy silt with coarser lenses of sand and basal pebbles. I sampled four sites on the south side of the incised channel and two sites on the north side of the channel.

Lola

Upstream and on the opposite bank of the Le Sueur from Leigh, Lola is situated on a low terrace of the river. It possesses more traditional ravine characteristics of the LSRB with a single channel headcutting into the valley wall, ongoing incision, and a radial alluvial fan. The channel incises more than two meters into the fan apex to the culvert where it enters the Le Sueur. The landowner often complains of sediment pulses that frequently bury his fire pit at the ravine base. The alluvial fan is built on a filled-in oxbow channel, and the close proximity of the water table often interfered with augering operations. The owners planted an orchard on part of the fan, and a portion of it is abandoned agricultural fields. Three transects radiate out from Lola 2 in the center of the fan with Lola 1 at the apex.

Loren

Loren is a multi-branching ravine with three main channels. It has a small creek flowing through the northern branch of the ravine that flows out onto its alluvial fan and into a ditch where it reconnects to the Le Sueur River. Near its apex, it has incised up gradually to 2.66 meters, but incision depth dissipates in the headward direction until the main ravine channel is flowing on the mucky, silty surface. Loren has an alluvial fan on the terrace, now developed with buildings and an orchard. Loren is the exception to the rule where I sample on alluvial fans. Although its alluvial fan fits the qualifications for my field sites, my sampling occurred in the ravine above the fan apex because the ravine appears to be filling itself in. The elevation and slope of the filled-in ravine easily transitions into the alluvial fan. The valley is disproportionately wide compared to other ravines, and lacks significant incision. The valley wall slopes in the ravine are shallow enough to render sediment stable from mass movements due to canopy cover and vegetation undergrowth; however, the ravine valley is vegetated only with seasonal stinging nettles and grasses.

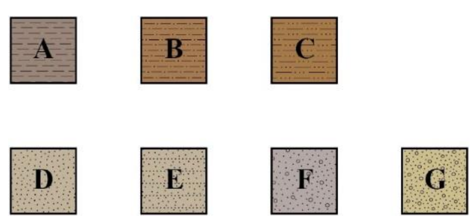

Figure 7a-f. Stratigraphic columns from transects on sampled sites, and identification key above for grain size classification. A-silt, B-sandy silt, C-silty sand, D-massive sand, E-bedded sand, F-sand and granule, G-sand and gravel.

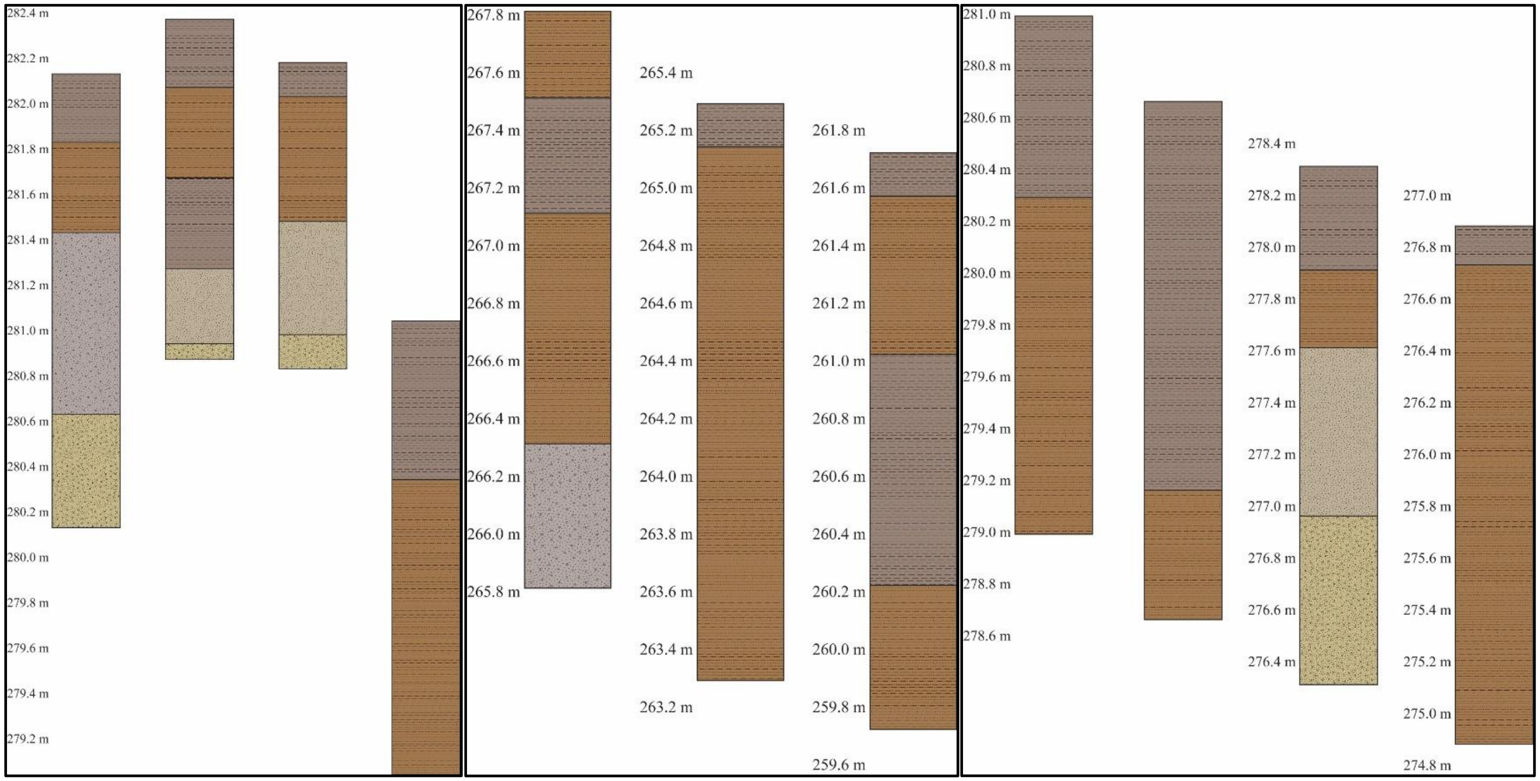

Figure 8. Incised alluvial fan stratigraphy.

Column numbers from left to right:

a) Mel 1, 2, 3, and 4

b) Magdalena 3, 5, and 7

c) Catalina 3, 4, 5, and 6

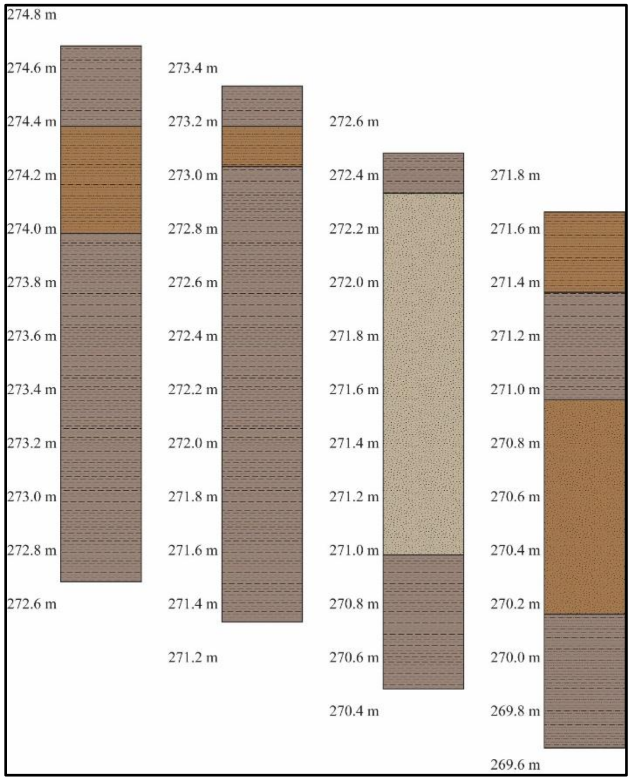

d) Leigh 4, 1, 2, and 3

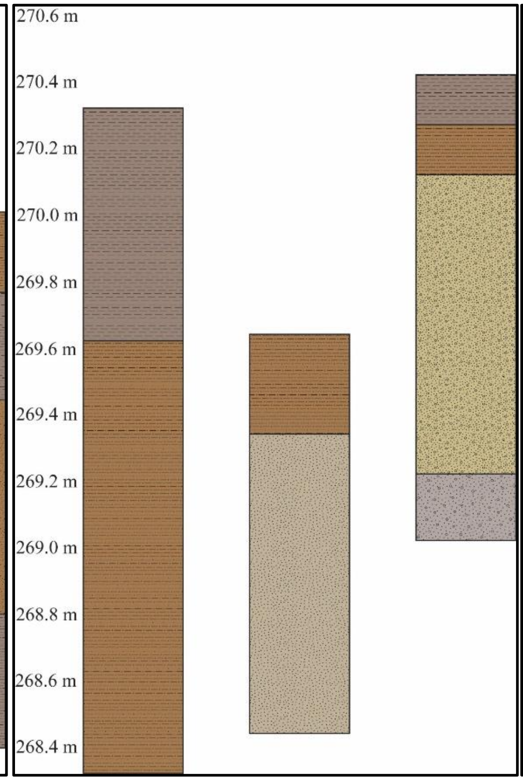

e) Lola 2, 4, and 5

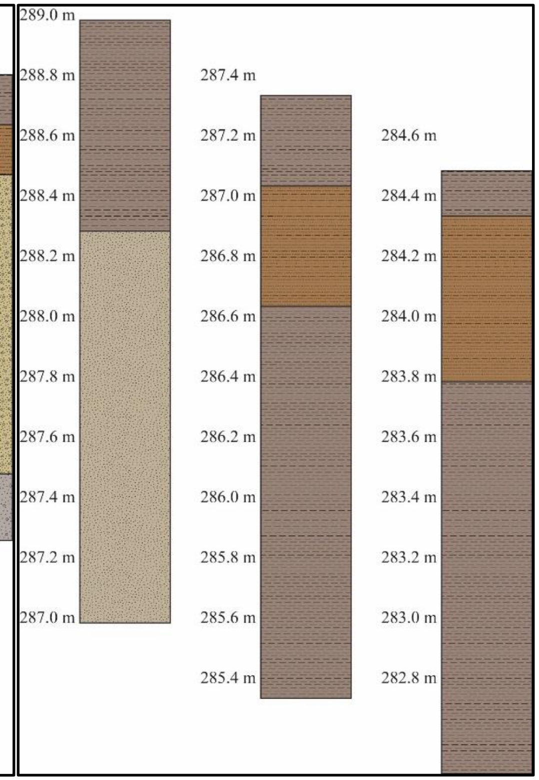

f) Loren 5, 4, and 3

Alluvial Fan Stratigraphy

Basin-wide alluvial stratigraphy follows a similar template: Most of the top 150-centimeters is a mixed sandy silt with a coarser base ranging from sand to pebble size. Alluvial exposures in the incised channel show similar patterns to the sediment as classified from the auger holes. The depth of incision varied from fan to fan.

Access within an incised channel allowed me to see stratigraphy clearly in the dissected fans. I recorded grain sizes from every dried sample that I collected on the alluvial fans, and I assembled stratigraphic columns after completing grain size analyses. One consistent pattern across the basin is the fining-upward sequences (Figure 7a-f). Some fans had layered dark gray clays below sandy layers. Both Leigh and Lola exhibited this (Figure 9). Mel had an almost impenetrable layer of gravel at depths throughout the fan. It took multiple attempts to collect the 200-centimeter auger sample. It was difficult to sample on Lola because the water table was so close to the surface, especially on the fringes of the fan. A slurry of sediment was removed from the bore holes at far-reaching locations from the apex at depths greater than 150-centimeters. The fan is built on an old oxbow, which explains the shallow water table. Although not recorded in the sediment column, Leigh had thick basal gravel layers at 440-centimeters deep (Figure 10). This posed a problem later when I discovered fly ash below these gravels calling into question the integrity of fly ash as a stratigraphic marker at this site.

Although true coarsening-upward sequences are not the case on every fan, some fans alternate between coarse and fine sediments. The grain sizes of the coarser layers varied at sites. Magdalena was hard to categorize because it had the steepest fan slope—almost as if it was built as a series of landslide or debris flow events, yet much of the fan is fine-grained.

Even Leigh, which had coarse basal layers near the bottom of the fan, was relatively fine-grained in the auger samples. Ideally, coarse material should congregate at greater depths near the apex of the fan. That is not always the case. Mel and Magdalena are the only two where there is coarser material at the apex of the fan. Other fans have coarse sand-sized or greater material at the edges.

Figure 9. Dark gray clays on Leigh and Lola below sandy layers.

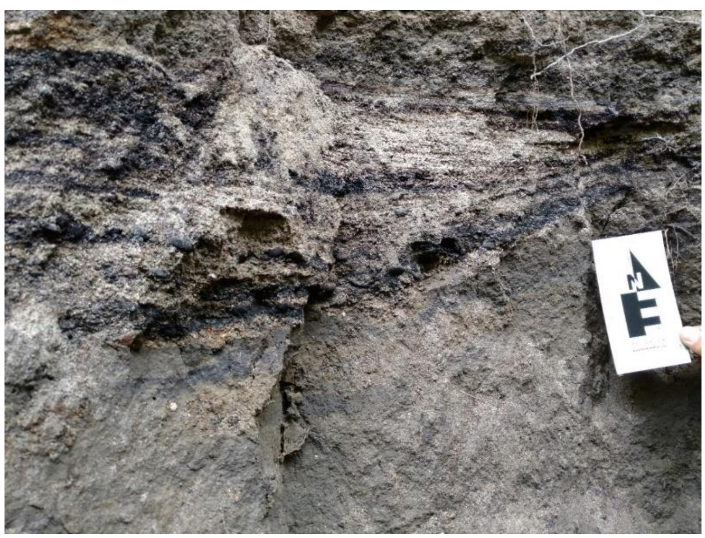

Figure 10. Thick gravel layers bedded above clay layers on Leigh in the incised channel.

Lidar Observations

Lidar was flown over Blue Earth County in 2005 and again in 2012. Schaffrath et al., (2012) calculated the DEM of Difference (DoD) from the two flights. I used the data to calculate ravine headcut migration and alluvial fan incision depths within the LSRB. With the DoD data, I was able to calculate net volumetric erosion for the six studied ravine and alluvial fan polygons at 1.92 x 10^5 m^3 (Figure 11).

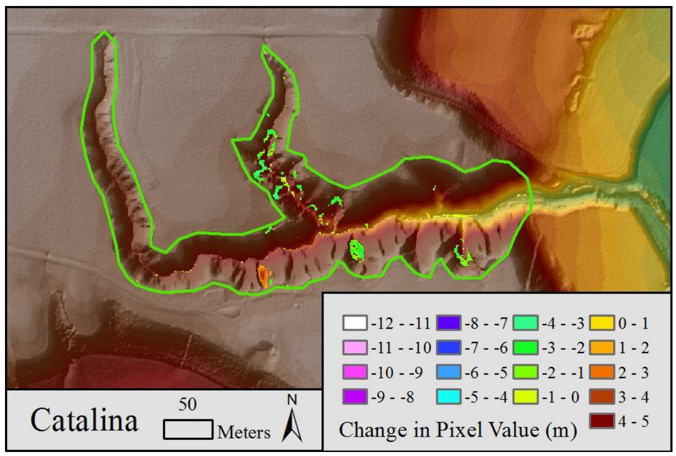

Figure 11. DEM of Difference (DoD) values used from Schaffrath et al., (2015) to calculate volumetric erosion and deposition on the sampled ravines and alluvial fans.

Post-Settlement Alluvium Results

The depths of fly ash within the alluvial fans appear to vary based on location. Basin-wide, the average thickness of sediment containing fly ash on alluvial fans is 135 centimeters, ranging from 95 to 157 centimeters across six sampled alluvial fans by the presence-absence method. My development of the three surveys fills in apparent gaps in the fly ash record. In the presence-absence survey, fly ash concentrations appear to be trace but present, particularly in upper samples. The basin-wide average maximum depth at which fly ash is found based on the presence-absence test is 135-centimeters (Figure 12). Fly ash depth was compared with several independent variables including distance to Mankato, terrace age, fan evolution stage, and fan size. There is no correlation among the variables, but the strongest trends were found comparing fly ash depth to fan size (Figure 13). The larger the fan size, the deeper the average fly ash maximum depth.

The highest-resolution survey conducted on the fans was using the SEM. I took photographs and saved EDS reports on elemental composition from all the fly ash grains in the samples. Because these samples have such a thick background matrix of magnetic particles, the SEM was very helpful in finding and distinguishing fly ash from the matrix and from other particles that mimic its morphology and composition. Fly ash also weathers differently from two other ferruginous minerals, ilmenite and titanomagnetite. The high-resolution survey shows fly ash to be much more prolific among the matrix than appeared in the lower-resolution light microscope (Figures 14-16). Under the SEM, I determined fly ash abundance, mineralogy, and degree of weathering, which could be used as a proxy for age. Theoretically, intact grains appear at the top of the column, whereas, weathered grains are older and appear deeper down in the stratigraphy after undergoing chemical and mechanical weathering (Figures 17-18).

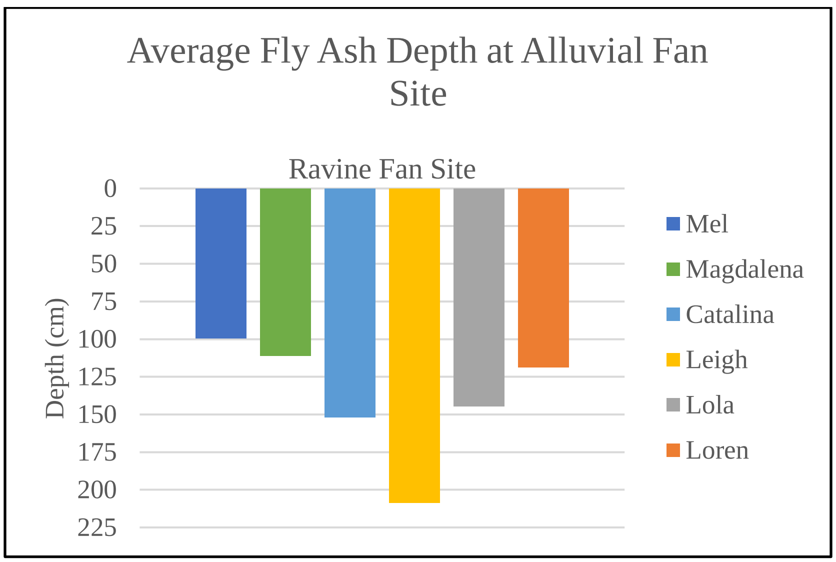

Figure 12. Average fly ash depths at each alluvial fan from the presence-absence survey

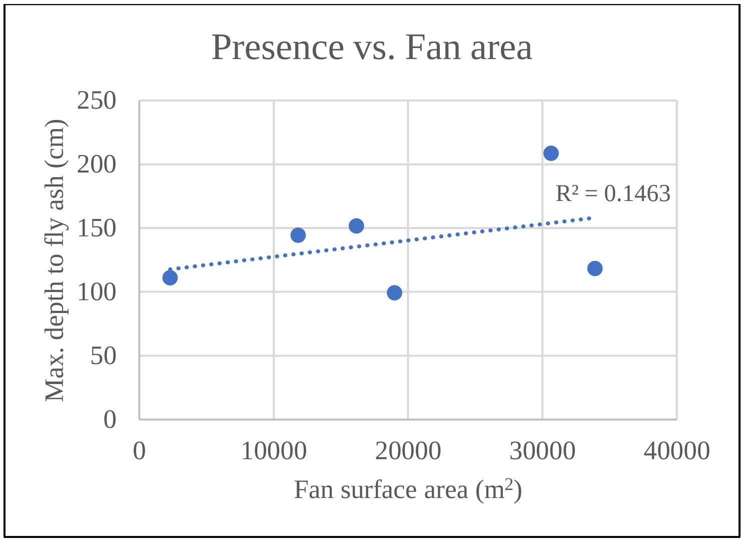

Figure 13. The strongest correlation between fly ash depth and an alluvial fan metric.

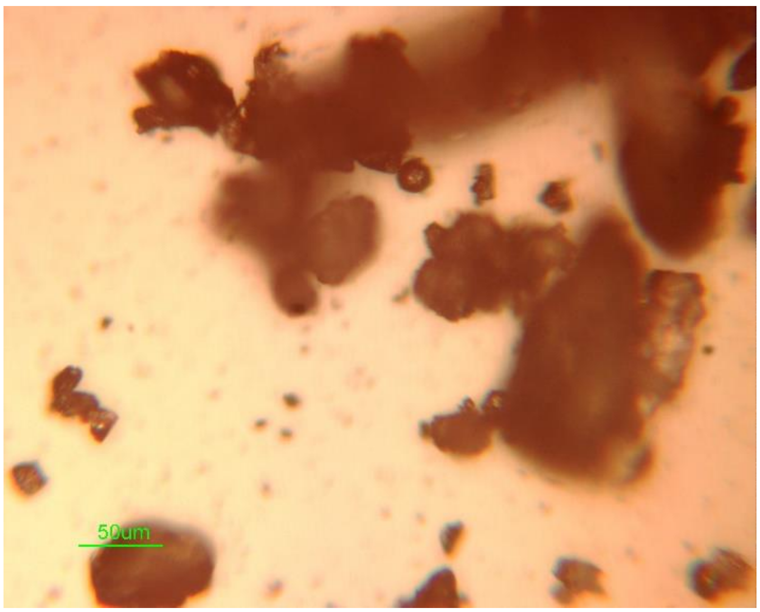

Figure 14. Visual light microscope analysis of fly ash (spherical particles).

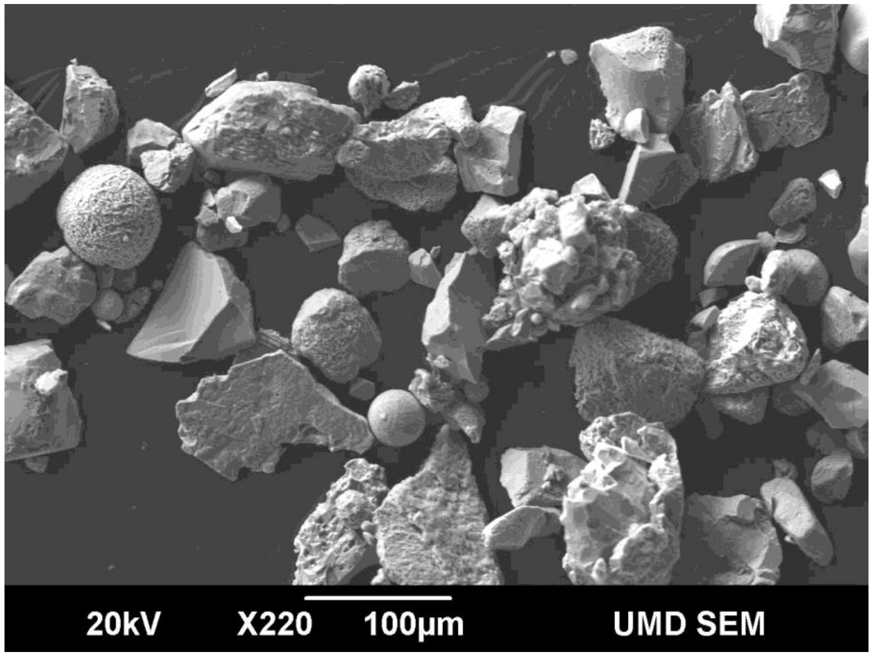

Figure 15. SEM photo at 220-x magnification from Loren 4 at 10-cm depth. Fly ash are the perfectly spherical particles in the center surrounded by natural magnetite, ilmenite, and titanomagnetite elsewhere.

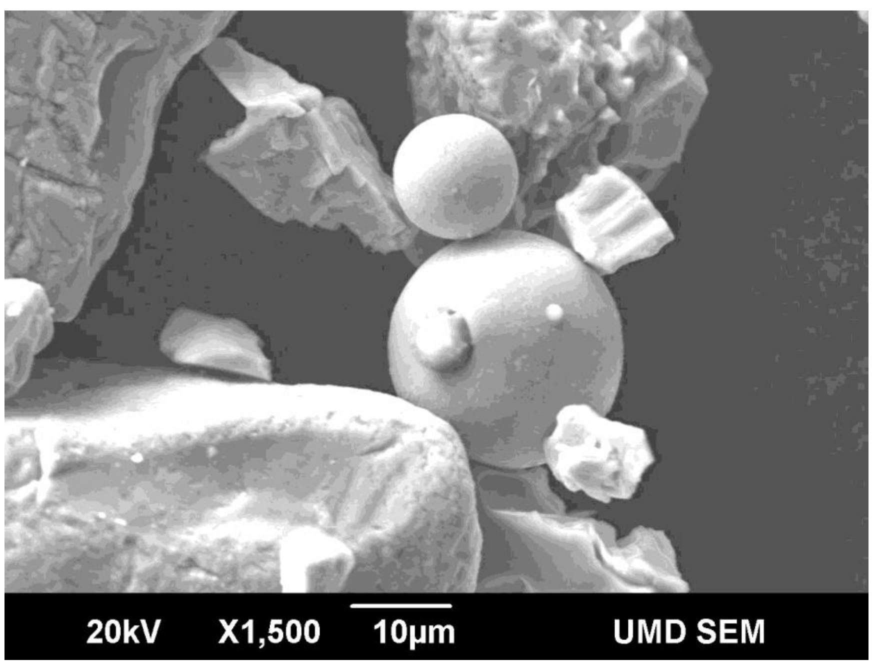

Figure 16. SEM photo at 1,500-x magnification from Leigh 4 at 10-cm. Fly ash particles are the two in the center surrounded by natural magnetic particles elsewhere.

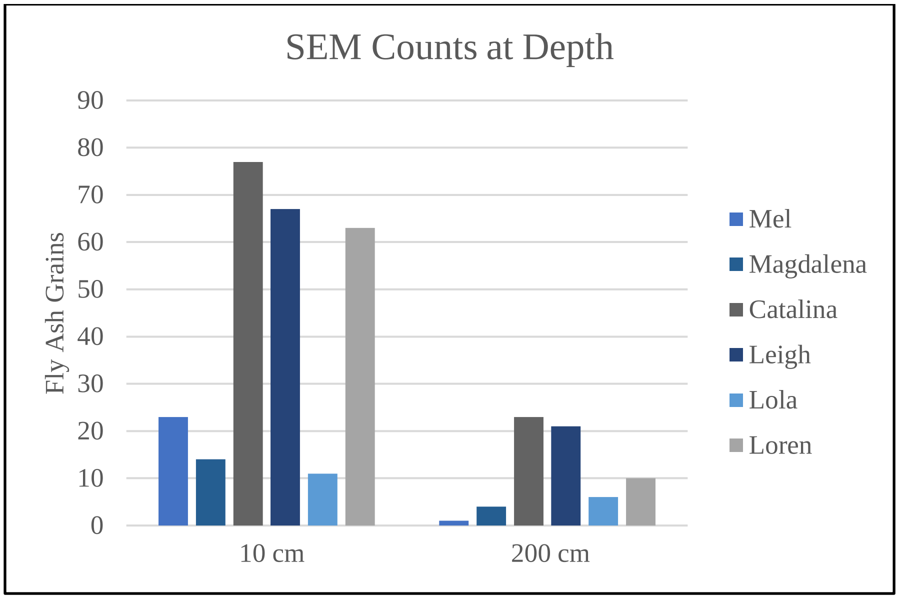

Figure 17. Number of fly ash grains at the top and bottom of each sampled location on the SEM survey.

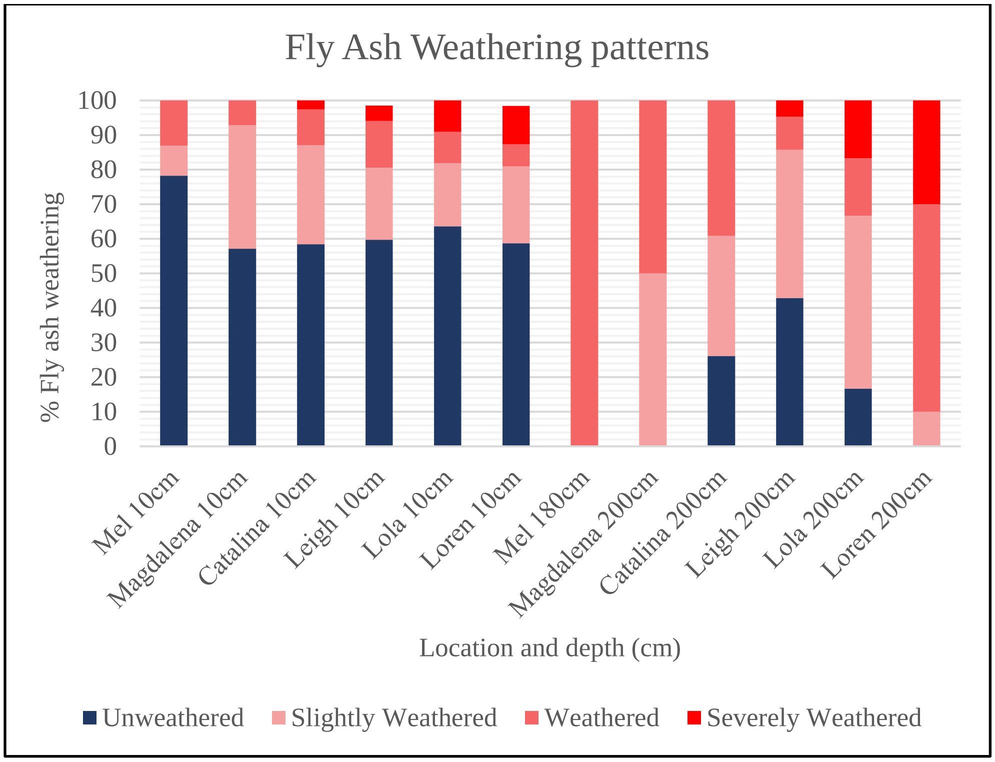

Figure 18. Normalized graph showing percentages of unweathered and different degrees of weathering at the top and bottom of SEM mounts.

Medium-resolution fly ash analysis takes the broad spectrum of fly ash presence and absence and modifies the inspection detail from the SEM technique. A curve showing fly ash density through depth in a fan emerged from the resultant data (Figure 19). The strongest peak is visible in the upper reaches of the sediment column. Fly ash weathering tends to be more weathered with increasing depth (Appendix 5).

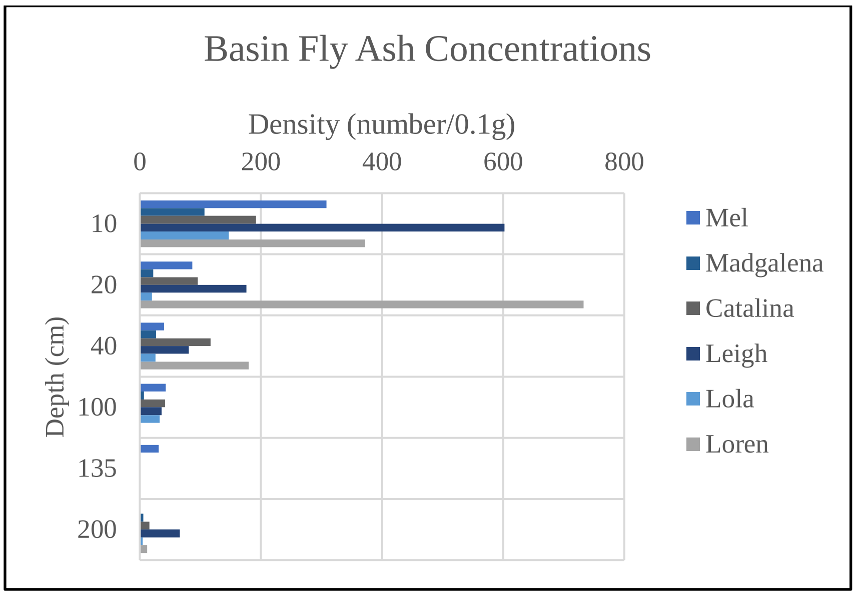

Figure 19. Normalized fly ash density versus depth from the modified visual light microscope survey.

Rate Calculations

Constraining historical fly ash production from railroads and industry and combining it with results from stratigraphic sediment analysis allows for the calculation of depositional rates from PSA marker beds to the surface. These calculations assume fly ash was produced from 1868 to 1970 with no changes in production rate or source change. The PSA deposition rate can be compared with sediment deposition rates going back to the age of the terrace. Table 5 illustrates how the incision depth at a fan apex divided by its respective terrace age can yield an estimate for a Holocene deposition rate. The most liberal estimates of Holocene deposition rates average 0.27 cm/yr with a standard deviation of 0.25 across five samples.

This assumes the maximum thickness of the alluvial fan (from the incision depth or the elevation difference of the fan) and divides it over the age of the terrace. Conservative rates from six site-averaged presence-absence surveys deposit sediment at 0.93 cm/yr with a standard deviation of 0.24 (Table 6). Lastly, rates from the six site-averaged SEM surveys estimate deposition to occur at 1.67 cm/yr with a standard deviation of 0.81 (Table 7). Rates will only be higher than these because the rates assume fly ash production was constant from 1868 to present. It also does not account for the time it took for the alluvial fans to experience re-incision. Even so, the most liberal Holocene deposition rates and the most conservative PSA deposition rates are not within error of each other. One caveat is that deposition rates can change without changing erosion rates by having a higher sediment retention efficiency on the alluvial fan. Conversely, erosion rates can change without deposition rates changing with higher sediment delivery ratios.

Erosion rates support post-settlement influences in the LSRB. Gran et al., (2009) calculated a background Holocene erosion rate by calculating the volume missing from the basin. Basin-wide, mass excavated from all ravines accounted for 2.2 x 10^8 Mg silt and clay. Over 13,500 years, that makes 16,300 Mg/yr or 0.0018 Mg/m^2/yr. Gran et al., (2011) calculates another Holocene erosion rate of 10,000 Mg/yr from all ravines, but the ravine loads are unconstrained with high uncertainties. From repeat lidar scans of Blue Earth County and the technique from Schaffrath et al., (2015), I calculated a net mass removed from the six sampled ravine polygons in ArcGIS of 331 Mg/yr for the years between lidar scans (2005-2012), which equates to 0.00118 Mg/m^2/yr. It worth noting that the level of detection (LoD) for the DoD was set at 29 cm, and net change within LoD could account for as much as 88,000 Mg, far exceeding the signal measured above LoD. I took the defined volumetric loss from GIS and multiplied it by the bulk density from Gran et al., (2009) to get a mass flux.

Table 5. Holocene deposition rates.

Ravine	A. Fan Thickness at Apex (cm)	B. Fan Incision Depth at Apex (cm)	C. Maximum Possible Thickness (cm)	Terrace Age (yr)	A. Deposition Rate (cm/yr)	B. Deposition Rate (cm/yr)	C. Deposition Rate (cm/yr)
Mel	470	330	470	3360	0.14	0.10	0.14
Madgalena	570	--	570	840	0.68	--	0.68
Catalina	380	780	780	1430	0.27	0.55	0.55
Leigh	330	760	760	4020	0.08	0.19	0.19
Lola	310	210	310	9250	0.03	0.02	0.03
Loren	490	230	490	7870	0.06	0.03	0.06
				Average Deposition Rate (cm/yr)	0.21	0.18	0.27
				Standard Deviation	0.22	0.19	0.25

A. takes the maximum thickness of the fan at its apex and calculates a deposition rate from the terrace age; B. calculates a deposition rate from subtracting the terrace elevation from the elevation of the apex; and C. takes the greatest rate from A and B to calculate the most liberal deposition rate for the Holocene.

Table 6. Presence-Absence PSA deposition rates.

Ravine	Average Maximum Fly Ash Depth (cm)	A. Likely Fly Ash Production (yr)	B. Reasonable Fly Ash Production (yr)	C. Conservative Fly Ash Production (yr)	Deposition Rate A (cm/yr)	Deposition Rate B (cm/yr)	Deposition Rate C (cm/yr)
Mel	99	80	102	150	1.24	0.97	0.66
Magdalena	111	80	102	150	1.39	1.09	0.74
Catalina	152	80	102	150	1.90	1.49	1.01
Leigh	209	80	102	150	>2.61	>2.04	>1.39
Lola	145	80	102	150	1.81	1.42	0.96
Loren	119	80	102	150	1.48	1.16	0.79
Average Depth (cm)	139			**Average Deposition Rate (cm/yr)**	1.74	1.36	0.93
				Standard Deviation	0.45	0.35	0.24

The average maximum fly ash depths are divided by the length of fly ash production, which yields three PSA deposition rates. The most conservative rate is 0.93 cm/yr.

Table 7. SEM PSA deposition rates.

Ravine	Average Maximum Fly Ash Depth (cm)	A. Likely Fly Ash Production (yr)	B. Reasonable Fly Ash Production (yr)	C. Conservative Fly Ash Production (yr)	Deposition Rate A (cm/yr)	Deposition Rate B (cm/yr)	Deposition Rate C (cm/yr)
Mel	180	80	102	150	2.25	1.76	1.20
Magdalena	200	80	102	150	2.5	1.96	1.33
Catalina	200	80	102	150	2.5	1.96	1.33
Leigh	520	80	102	150	>6.5	>5.10	>3.47
Lola	200	80	102	150	2.5	1.96	1.33
Loren	200	80	102	150	2.5	1.96	1.33
Average Depth (cm)	250			**Average Deposition Rate (cm/yr)**	3.13	2.45	1.67
				Standard Deviation	1.51	1.19	0.81

There is one additional anthropogenic marker for settlement in the LSRB. When removing sediment from the auger to sample a site on Loren at 200-centimeters, a heavily oxidized metal staple fell out of the auger (Figure 20). That could only come from an anthropogenic source. Its size effectively renders it immobile once buried in the sediment. Because fly ash was present above and below this marker, I have strong reason to believe that this helps build confidence in fly ash as an accurate PSA marker.

Figure 20. Rusted metal pin from auger on Loren.

Discussion

Ravine alluvial fans in the LSRB are sensitive erosive features. Base-level adjustment from the drainage of Lake Agassiz during glacial retreat initiated incision. Land use change led to decades of further instability depositing upwards of two meters of PSA on the six sampled alluvial fans. Fly ash in stratigraphy was successful in placing PSA in the greater context of the alluvial fans. Other in situ physical markers such as the metal pin in Loren aided in stratigraphic inferencing.

Settlement Effects on Alluvial Fans

Multiple stage alluvial fan evolution signifies the fast response times that ravines have for anthropogenic alterations. Ravines are active systems with steep sidewalls and headcuts with incising channels. Land use changes, such as agricultural plowing, forest clearing, and drainage, compounded upon existing ravine instability. Further instability increased deposition rates on alluvial fans, likely due to increased erosion in ravines. Although Holocene deposition rates are not as well constrained as post-settlement rates, applying post-settlement rates over the age of the fans leads to unreasonable sediment thicknesses. For instance, if we take the presence-absence survey deposition rate of 1.36 cm/yr and apply it to Mel on a 3,360-year-old terrace that yields fan sediment thicknesses of 45.7 meters, which we do not see. Additionally, sediment thicknesses with 2.45 cm/yr of deposition from the SEM survey yields 82.3 meters. Ravines have a tight connection between an increase in erosion rates and an increase in deposition rates. Ravine alluvial fans respond and archive the changes from inputs in evolutionary stages. Initial clearing of the ravines and prairie plowing sent pulses of sediment down the ravines and on top of alluvial fans evidenced by thick packages of PSA deposits found across the fan surfaces cored. Physical objects and fly ash are also found in alluvium.

After ravines revegetated from the initial land clearing, ditches and tile drainage were installed to drain the fields. Ravines responded to this increased hydrologic flux by transporting more sediment and excess water down onto alluvial fans. In some ravines, excess water incised through fan surfaces instead of building larger alluvial fans. Deeply incised channels work their way headward into the fringes of ravines. Incision episodes are visible after rainstorms resulting in meters of upstream incision, or headcutting, some of which incise through the alluvial fan and terrace material.

Because erosion and deposition in this system are precipitation-driven, alluvial fans build in pulses just like incision occurs after storm events. This is visible in the LSRB and in the neighboring Blue Earth River. Numerous residents commented on the rate of ravine change and their ability to expand rapidly. Residents on Mel noted how rapid the ravine expanded and incised; whereas, residents on Lola complained of large sediment pulses disturbing their property. While it may seem like these are contradictory accounts to the overarching hypothesis, the common denominator in this basin is that these events occur rapidly. Whether a ravine is experiencing erosion versus deposition is both a function of water and sediment balances through the ravine and the sampled location on the fan surface. Again, alluvial fans on one ravine may be experiencing a different evolutionary stage than another alluvial fan. Their response is shifting the balance between hydrologic and sediment fluxes.

Grimley et al., (2017) shows an increase in magnetic susceptibility as the depths shallow until the very top where there is a drop off in floodplain alluvium in Illinois. Figure 19 highlights a different pattern in ravine alluvium in the LSRB, with fly ash concentrations increasing all the way up to the highest sample (10cm). The implementation of the Clean Air Act in 1970 stopped the release of airborne fly ash into the atmosphere thereby cutting off the source of fly ash. In the floodplains of Illinois, this led to a decrease in fly ash in the most recent deposits, but not so on the ravine fans where the highest concentrations of fly ash are found at 10 cm on five of the six fans. Either deposition switched to incision on the alluvial fans during peak fly ash production, or eroded material from the ravine or uplands with fly ash continues to deposit on the surface.

Ravines in a Changing Climate

Anthropogenic changes manifest themselves as depositional packages followed by re-incision resulting from land use changes on the uplands and in the ravines, showing the sensitivity of these ravine systems to external perturbations. Headcutting and alluvium deposition are frequent during and after storms. These changes are accentuated by large storms. Several large precipitation events occurred in the last decade. The LSRB has experienced two 100-year floods and two 25-year floods causing widespread sediment transport and property damage (Table 8). On the uplands, human-induced changes wring the water out of the land by ditching and drain tile installation. Now, because of a changing climate, we see the effects of intense precipitation events and resulting large floods. Geomorphically-sensitive regions modified by human influences might feel the effects of climate change first (Novotny and Stefan, 2007; Lang et al., 2013; Kelly et al., 2017). I witnessed several meters of headcutting after a 10-centimeter rainstorm—far less precipitation than that leading to a 100-year flood.

Table 8. Le Sueur River flood statistics.

Date	**Year**	**Discharge (cms)**	
9/26/2010	2010	864	
4/8/1965	1965	699	
5/22/1960	1960	600	
9/24/2016	2016	555	100-year flood threshold
6/21/2014	2014	442	25-year flood threshold
3/21/2011	2011	402	
4/7/1951	1951	374	
4/6/2001	2001	371	95% confidence interval 25-year flood

Technique Assessment

One of the objectives of this study was to determine if the fly ash technique works in alluvial fans like it did in floodplain alluvium in Illinois where it was developed. Fly ash stratigraphy in alluvial fans aids us in our understanding of co-evolving ravines and alluvial fans. It works well as a stratigraphic marker in oxidizing fluvial systems where other traditional stratigraphic markers like pollen may not be as well preserved. Distance from the source, means of sediment deposition, and incision and abandonment of fan surfaces were the three variables that required me to modify fly ash techniques from Grimley and Arruda (2007).

Fly ash densities within the dried fraction were sparser than the concentrations measured by Grimley and Arruda, (2007) in Illinois floodplain alluvium. Where they counted 15 to 20 fly ash grains per 100, I counted less than one. The apparent low fly ash density made me change the technique. The SEM was extremely useful when viewing fly ash up close; otherwise, most of the visual light microscope point counts would be trace. The discrepancy was from our distances from fly ash sources. Where they sampled directly next to a power plant, I sampled several kilometers away from railroads and Mankato. The alluvial fans relied on winds to blow fly ash from a passing train and industrial plants (Jones and Olson, 1990) or concentrated flow to transport material down from the uplands (Hussain et al., 1998). Even so, I could detect fly ash, but the abundance was much lower. The abundance of sediment from in-ravine erosion could have diluted fly ash populations as well.

The frequency and spatial variability of deposition also affects fly ash concentrations. Alluvial fans receive flashy flows from the ravines that deposit sediment in packages. They depend on precipitation from storms to deposit sediment on fan surfaces. Fly ash deposited in floodplain alluvium in the study by Grimley et al., (2017) is also precipitation-dependent as the river rises and falls from storm events, albeit, not as flashy as ravines. Deposition on a floodplain surface is more widespread than deposition on a fan surface, especially for the fine fraction. Amongst the alluvial fans, some are finer than others (Figure 7).

Incision through alluvial fans disrupts the depositional history of fly ash in the LSRB.

We attribute rapid re-incision of the alluvial fans to increased discharge through ravines from altered hydrology (tile drainage) on the uplands coupled with increasing precipitation and intensity of precipitation (Novotny and Stefan, 2007; Schottler et al., 2013; Foufoula-Georgiou et al., 2015). This poses difficulty in bracketing the youngest fly ash in sequence. Incision may have started through the fan before 1970 with the implementation of the Clean Air Act—requiring coal-fired power plants to install scrubbers eliminating the production of most fly ash—and essentially ceasing deposition on some alluvial fans. Steam trains were phased out earlier in the 1940s and 1950s with diesel locomotives. Percent fly ash and magnetic susceptibility reduce dramatically in Grimley et al., (2017)'s study area in Illinois. There are no incidents of incision through floodplain alluvium in Illinois; however, storm-driven periodic deposition kept alluvium thicknesses relatively uniform, and the youngest fly ash is found at the top of the stratigraphy. In the LSRB, depth to fly ash is not uniform. Some ravines are more active than others, yet fly ash is always at the top of each sediment sequence with a drop off in concentration with increasing depth (Graph 5). Because of differences in depositional setting and fly ash sources, abundances were much lower in the LSRB. This required developing new techniques.

Comparison of Techniques

The presence-absence survey does not quantify results. It is a purely qualitative analysis of fly ash existence within the ravine's alluvial fan. Since I did not have EDS analysis at my aid for this survey, I made judgments of fly ash solely off its morphology. I had photographs and experience looking at it while learning this technique, but ilmenite and magnetite are indistinguishable under a visible light microscope.

I was uncertain about which grains were fly ash in the first survey until I investigated the samples under the SEM. Clearer image resolution and EDS analysis identified magnetite fly ash against the background of crystalline magnetite and other magnetic minerals. Counting each grain was cumbersome but necessary to constrain population densities. The population densities, when defined, are clear markers for post-settlement alluvium.

Static attraction within these communities of magnetic fraction often harbor interstitial fly ash. It is easy to focus in and out of these population centers on the electron microscope, but on the visual light microscope, interstitial fly ash gets lost in the topography (Figure 21). Lateral panning around the cube was no longer sufficient to quantify fly ash. I had to vertically pan up and down the topographic variation in the magnetic fraction. Fly ash was more visible after that adaptation. This medium resolution survey made visible any patterns that were not visible because of lack of resolution in the presence-absence survey, and it filled in gaps in data in electron microscope analysis.

To determine future PSA horizons, one suggestion would be to sample soil for Cs-137 content. That would add a viable midpoint for places where fly ash had a wide date range for production. Use magnetic susceptibility as a control for fly ash presence. The plots for fly ash concentrations versus magnetic susceptibility of soils should look similar (Grimley et al., 2017). For future use of fly ash, I recommend using the SEM first as pilot samples at the top and bottom of sediment columns. That way it familiarizes the observer with the morphology of fly ash and its mimicking particles as well as its elemental composition. Then I would move to the visual light microscope and scan the topography in the fly ash carefully for statically-attracted grains as fly ash often hides interstitially.

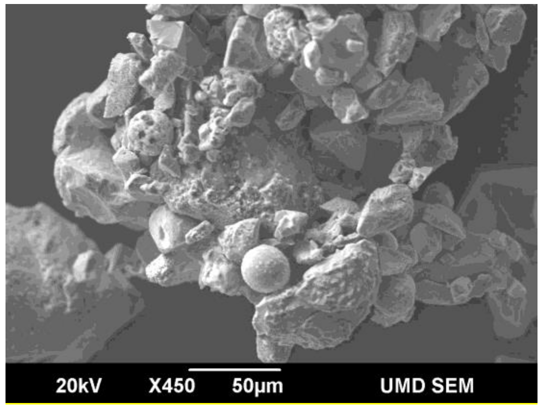

Figure 21. This picture illustrates the topography found in fly ash. It clusters together and is difficult to spread out on SEM mounts and the plastic analytical cubes.

Conflicting data

The results section outlined a conflict between a couple radiocarbon dates in alluvial fans and fly ash in the stratigraphic column. Accurate, in-situ radiocarbon dates create problems with fly ash accuracy. Alternatively, fly ash highlights a potential problem with obtaining in-situ radiocarbon dates that do not contain old carbon. At Leigh 440-centimeters below the fan surface, I found fly ash in dark, silty material directly below a basal gravel layer (Figure 9). These clay deposits might be late slackwater deposits as the river abandoned the floodplain, and the alluvial fan began to build onto the terrace. There may be several iterations of these inter-lobed events not visible in the examined stratigraphy that are buried elsewhere in the fan. Above this sample at 180-centimeters below the surface, there is carbon-rich soil and charcoal flakes dated at 3710 ± 30 yr BP. In a similar dark, silty material on Mel, we dated charcoal at 300 ± 30 yr BP in the incised channel at the apex of the alluvial fan. Fly ash was found at both of these locations, meaning there is a possibility that, if the carbon-rich material is in situ and does not contain recycled older carbon, fly ash percolated down through the soil. Discrepancy between the age dates can be explained by considering a two end-member hypothesis. The first end-member assumes the radiocarbon date is accurate, which means groundwater, bioturbation from roots, or burrowing insects or animals transported fly ash more than three meters down through the stratigraphy. This undermines the reliability of fly ash as a stratigraphic marker for PSA surfaces in porous media, and casts doubt into the accuracy of other fly ash observations in the basin. The second case is that, considering the erosive potential of the ravines, the age is legacy carbon reworked into alluvium; therefore, the date can be negated and the fly ash considered in-situ.

Alluvial fans in temperate environments are relatively porous (Kehew et al., 1996), so it is reasonable to assume that silt-fraction fly ash is easy to transport through in groundwater. However, its appearance within the dried fraction under a microscope is clustered with other magnetic minerals. Fly ash congregates within the dried fraction statically or magnetically, which may make it more difficult to transport in porous material. Both end members are relatively extreme with their transportation (or lack thereof) of fly ash.

Fly ash as a silt-sized particle might be transported down through a soil column as part of pedogenic processes. The depth of a B-horizon indicates the likelihood of silt or clay particles to translocate down a column through eluviation. Deep B-horizons show that clays can move farther down the column, whereas, shallow horizons do not support the long range motion of fines. The presence or absence of B-horizons also indicates the age of soil or rate of deposition. The absence of a B-horizon altogether means the soil has not matured, common in cumulic soils with high deposition rates. Locating B-horizons in alluvial fans infers the surface has remained at that level long enough for a B-horizon to form at depth. Evidence for deep pedogenesis implies that, given enough time, silt- and clay-sized particles could translocate down to the depth at which B-horizons formed.

Using the NRCS Soil Survey web application, I researched soil profiles for the six alluvial fans I sampled (Appendix 7). Of the six alluvial fans, Mel, Catalina, and Loren exhibit the A-C-A horizon pattern indicating buried or cumulic soils. Deposition occurred rapidly on Mel, Catalina, and Loren when they were accumulating alluvium. Magdalena, Leigh, and Lola have B-horizons in their profiles beginning at 53-, 86-, and 38-centimeters depth, respectively (Natural Resource Conservation Service). The soil profile for Magdalena from the NRCS notes was taken on the terrace it deposits on because it is such a small feature. This explains the B-horizon on the terrace meaning the alluvial fan itself is cumulic. These depths are where, over time, fly ash-sized particles could translocate down through the soil column and accumulate. In the field, Lola exhibited some color lightening and oxidation.

Technique Suggestions

While I still consider fly ash to be an accurate technique for PSA analysis in temperate alluvial fans, there are a few suggestions I would make for those considering this technique. Bring a hand auger that is long enough to drill through the alluvial fan thickness, and sample at equal intervals to capture any gradient in fly ash deposition. I also caution sampling near locations that may have induced high hydraulic conductivity as this may potentially give false fly ash depths. Within temperate alluvium, fly ash results would be enhanced paired with other techniques such as magnetic susceptibility (Kapicka et al., 1999; Grimley et al., 2004; Grimley and Arruda, 2007; Grimley et al., 2017), radiocarbon dating, optically-stimulated luminescence (OSL), and Cesium-137 isotope analysis. Finally, establish a post-settlement marker fly ash concentration.

Conclusion

The dynamic history of the knickpoint migration and channel incision on the main stem rivers in tributaries of the Minnesota River basin affected the ravines and sediment storage in numerous ways. It created steep incising features. On-going incision of main stem channels has maintained ravines and extended the tips headward, but lateral migration of channels occasionally stranded the ravines, leading to deposition on terraces and a potential period of healing and stasis in the ravines. Within the main river valleys, base-level readjustment and knickpoint migration led to narrow floodplains with little sediment storage. This eliminated traditional sinks for fluvial sediments in the LSRB. Lateral meander migration and terrace formation thus created one of the few potential storage areas where alluvial fans deposited sediment. Deposition continued throughout the Holocene until the arrival of Euro-American settlers in the mid-1800s when conditions changed.

The arrival of Western settlers brought land use change on the uplands and in the ravines. Clear-cutting of the ravines for wood and plowing of the upland prairies for agriculture altered the sediment and hydrologic fluxes in the basin. Destabilization of the soil sent packages of sediment down through the ravines and onto the terraces. When the sediment load exceeded the transport capacity, post-settlement alluvium was deposited on top of Holocene alluvium. Ravines revegetated and drainage ditches and tiles were installed on farm fields, and residence time decreased when rain fell on the fields. The resulting increase in transport capacity caused incision that dissected many alluvial fans in the LSRB. This is a common pattern throughout the basin, with some alluvial fans and ravines experiencing cycles of aggradation and incision from individual storm events. Several ravines were reconnected to the mainstem rivers, which also led to a wave of headward incision.

Post-settlement alluvium packages are marked by fly ash—a bi-product of coal combustion. Chronologically-constrained production means that fly ash in situ represents a depositional surface. Basin-wide, the average thickness of sediment containing fly ash on alluvial fans is 135-centimeters ranging from 95 to 157-centimeters across six sampled alluvial fans. Using a fly ash window from the arrival of railroads to the present yields a conservative PSA deposition rate of 0.93 cm/yr. Since peak fly ash production was from the 1880s to the 1950s, the deposition rate may be as high as 3.13 cm/yr from the SEM survey, or even higher if incision occurred, ceasing deposition on the alluvial fan surfaces and focusing flow through the incised channel.

Re-incision through an alluvial fan is a result of hydrologic change, driven by both land use change and climate change (Schottler et al., 2013). The incised channels expose stratigraphy in the alluvial fans and provide sampling locations. Since the arrival of railroads 150 years ago, ravines have deposited at least two meters of PSA in some locations, and in places, have eroded through all of it exposing older alluvium and terrace deposits.

This study quantified PSA using fly ash as a stratigraphic marker. The extraction and analysis techniques transitioned easily from floodplain alluvium, from which they were developed, to ravine alluvial fans, with some adjustments due to a lower overall abundance of fly ash in the alluvial fan deposits studied here. The three surveys I used to adapt to the lower abundance in fly ash density complement each other because they cover different resolutions of fly ash information on the basin. Coarse-resolution presence-absence surveys quickly identify fly ash in alluvium from many samples. It is helpful with the overview of fly ash in the basin. Fine-resolution surveys from the SEM and EDS are crucial for confirming fly ash from the dried fraction and allowing for the most accurate point count. It is the most important of the surveys because of its clarity and accuracy; however, it is the most time-consuming. Finally, medium-resolution analysis under the light microscope bridged the gap between the broad, shallow survey and the narrow, deep survey. It provided insight into PSA depositional trends evidenced by fly ash in select locations.

References Cited

Belmont, P., Gran, K.B., Schottler, S.P., Wilcock, P.R., Day, S.S., Jennings, C., Lauer. J.W., Viparelli, E., Willenbring, J.K., Engstrom, D.R., Parker, G., 2011, Large shift in source of fine sediment in the upper Mississippi River. Environmental Science and Technology, 45, 8804-8810.

Blue Earth County Historical Society. Phone Conversation.

Bogemans, F., Meylemans, E., Jacops, J., Perdaen, Y., Storme, A., Verdurmen, I., DeForce, K., 2012, The evolution of the sedimentary environment in the lower River Scheldt valley (Belgium) during the last 13,000 a BP. Geologica Belgica, 15, 105-112.

Bull, L.J., Kirkby, M.J., Shannon, J., Hooke, J.M., 1999, The impact of rainstorms on floods in ephemeral channels in southeast Spain. Catena, 38, 191-209.

Burkard, M.B., Kostaschuk, R.A., 1995, Initiation and evolution of gullies along the shoreline of Lake Huron. Geomorphology, 14, 211-219.

Campbell, I.D., 1999, Quaternary pollen taphonomy: Examples of differential redeposition and differential preservation. Palaeogeography, Palaeoclimatology, Palaeoecology, 149, 245-256.

DeRose, D.C., Gomez, B., Marden, M., Trustrum, N.A., 1998, Gully erosion in Mangatu Forest, New Zealand, estimated from digital elevation models. Earth Surface processes and Landforms, 23, 1045-1053.

Dotterweich, M., 2008, The history of soil erosion and fluvial deposits in small catchments of central Europe: Deciphering the long-term interaction between humans and the environment - A review. Geomorphology, 101, 192-208.

Engstrom, D.R., Almendinger, J.E., Wolin, J.A., 2009, Historical changes in sediment and phosphorus loading to the upper Mississippi River: Mass-balance reconstructions from the sediments of Lake Pepin. Journal of Paleolimnology, 41, 563-588.

Esteves, M., Lapetite, J.M., 2003, A multi-scale approach of runoff generation in a Sahelian gully catchment: A case study in Niger. Catena, 2003, 255-271.

Evans, D.J.A., Campbell, I.A., Lemmen, D.S., 2004, Holocene alluvial chronology of One Tree Creek, Southern Alberta, Canada. Geografiska Annaler, 86, 117-130.

Foufoula-Georgiou, E., Takbiri, Z., Czuba, J.A., Schwenk, J., 2015, The change of nature and the nature of change in agricultural landscapes: Hydrologic regime shifts modulate ecological transitions. Water Resources Research, 51, 6649-6671.

Gábris, G., Kertész, Á., Zámbó, L., 2003, Land use change and gully formation over the last 200 years in a hilly catchment. Catena, 50, 151-164.

Gran, K.B., Belmont, P., Day, S.S., Jennings, C., Johnson, A., Perg, L., Wilcock, P.R., 2009, Geomorphic evolution of the Le Sueur River, Minnesota, USA, and implications for current sediment loading. Geological Society of America Special Paper 451, 119-130.

Gran, K.B., Belmont, P., Day, S.S., Jennings, C., Lauer, J.W., Viparelli, E., Wilcock, P., Parker, G., 2011, An Integrated Sediment Budget for the Le Sueur River Basin.

Gran, K.B., Finnegan, N., Johnson, A.L., Belmont, P., Wittkop, C., Rittenour, T., 2013, Landscape evolution, valley excavation, and terrace development following abrupt postglacial base-level fall. Bulletin of the Geological Society of America, 125, 1851-1864.

Grimley, D.A., Arruda, N.K., Bramstedt, M.W., 2004, Using magnetic susceptibility to facilitate more rapid, reproducible and precise delineation of hydric soils in the midwestern USA. Catena, 58, 183-213.

Grimley, D.A., Arruda, N.K., 2007, Observations of Magnetite Dissolution in Poorly Drained Soils. Soil Science, 172, 968-982.

Grimley, D.A., Anders, A.M., Bettis III, A.E., Bates, B.L., Wang, J.J., Butler, S.K., Hout, S., 2017, Using magnetic fly ash to identify post-settlement alluvium and its record of atmospheric pollution, central USA. Anthropocene, 17, 84-98.

Gyssels, G., Poesen, J., Bochet, E., Li, Y., 2005, Impact of plant roots on the resistance of soils to erosion by water: a review. Progress in Physical Geography, 29, 189-217.

Hooke, J.M., 2006, Human impacts on fluvial systems in the Mediterranean region. Geomorphology, 79, 311-335.

Hooke, J.M., 2007, Monitoring morphological and vegetation changes and flow events in dryland river channels. Environmental Monitoring and Assessment, 127, 445-457.

Hussain, I., Olson, K.R., Jones, R.L., 1998, Erosion patterns on cultivated and uncultivated hillslopes determined by soil fly ash contents. Soil Science, 163, 726-738.

Jones, R.L., Olson, K.R., 1990, Fly Ash Use as a Time Marker in Sedimentation Studies. Soil Science Society of America Journal, 54, 855-859.

Kapička, A., Petrovský, E., Ustjak, S., Macháčková, K., 1999, Proxy mapping of fly-ash pollution of soils around a coal-burning power plant: A case study in the Czech Republic. Journal of Geochemical Exploration, 66, 291-297.

Kehew, A.E., Straw, W.T., Steinmann, W.K., Barrese, P.G., Passarella, G., Peng, W., 1996, Ground-water quality and flow in a shallow glaciofluvial aquifer impacted by agricultural contamination. Ground Water, 34, 491-500.

Kelley, D.W., Brachfeld, S.A., Nater, E.A., Wright, H.E., 2006, Sources of sediment in Lake Pepin on the Upper Mississippi River in response to Holocene climatic changes. Journal of Paleolimnology, 35, 193-206.

Kelly, S.A., Takbiri, Z., Belmont, P., Foufoula-Georgiou, E., *in review*, Human amplified changes in precipitation-runoff patterns in large river basins of the Midwestern United States. Hydrology and Earth System Sciences Discussions, 1-43.

Lang, A., Bork, H., Mäckel, R., Preston, N., Wunderlich, J., Dikau, R., 2003, Changes in sediment flux and storage within a fluvial system: Some examples from the Rhine catchment. Hydrological Processes, 17, 3321-3334.

Lass, W.E., 2011, Historical sketch of Mankato. The Northern Great Plains History Conference.

Lauriol, G., Lacelle, D., St-Jean, M., Clark, I.D., Zazula, G.D., 2004, The influence of biotic drivers on North American paleorecords: alternatives to climate. The Holocene, 14, 787-791.

Lewis, S.G., Birnie, J.F., 2001, Little ice age alluvial fan development in Langedalen, western Norway. Geografiska Annaler, 83, 179-190.

Li, Y., Xu, Q., Yang, X, Chen, H., Lu, X., 2005, Pollen-vegetation relationship and pollen preservation on the Northeastern Qinghai-Tibetan Plateau. Grana, 44, 160 171.

Locke, G., Bertine, K.K., 1986, Magnetite in sediments as an indicator of coal combustion. Applied Geochemistry, 1, 345-356.

Martínez-Casasnovas, J.A., 2003, A spatial information technology approach for the mapping and quantification of gully erosion. Catena, 50, 293-308.

Musser, K., Kudelka, S., Moore, R., 2009, Minnesota River Basin Trends. Water Resources Center, Minnesota State University, Mankato. Pp. 1-64. http://mrbdc.mnsu.edu/mnbasin/trends

Nagasaka, A., Yanai, S., Sato, H., Hasegawa, S., 2005, Soil erosion and gully growth associated with cultivation in southwestern Hokkaido, Japan. Ecological Engineering, 24, 503-508.

Natural Resource Conservation Service, Web Soil Survey. https://websoilsurvey.sc.egov.usda.gov/App/WebSoilSurvey.aspx

Nogueras, P., Burjachs, F., Gallart, F., Puigdefàbregas, J., 2000, Recent gully erosion in the El Cautivo badlands (Tabernas, SE Spain). Catena, 2000, 203-215.

Novntny, E.V., Stefan, H.G., 2007, Stream flow in Minnesota: Indicator of climate change. Journal of Hydrology, 334, 319-333.

Oostwoud Wijdenes D.J., Poesen, J., Vandekerckhove, L., Ghesquiere, M., 2000, Spatial distribution of gully head activity and sediment supply along an ephemeral channel in a Mediterranean environment. Catena, 2000, 39, 147-167.

Poesen, J.W., Vandaele, K., Wesemael, B.V.a.N., 1996, Contribution of gully erosion to sediment production on cultivated lands and rangelands. Erosion and Sediment Yield: Global and Regional Perspectives (Proceedings of the Exeter Symposium July 1996). IAHS Publ. 236, 251-266.

Poesen, J., Nachtergaele, J., Verstraeten, G., Valentin, C., 2003, Gully erosion and environmental change: Importance and research needs. Catena, 50, 91-133.

Rey, F., 2003, Influence of vegetation distribution on sediment yield in forested marly gullies. Catena, 50, 549-562.

Ries, J., Marzolff, I., 2003, Monitoring of gully erosion in the Central Ebro Basin by large-scale aerial photography taken from a remotely controlled blimp. Catena, 2003, 309-328.

Schaffrath, K.R., Belmont, P., Wheaton, J.M., 2015, Landscape-scale geomorphic change detection: Quantifying spatially variable uncertainty and circumventing legacy data issues. Geomorphology, 250, 334-348.

Schottler, S.P., Ulrich, J., Belmont, P., Moore, R., Lauer, J.W., Engstrom, D.R., Almendinger, J.E., 2014, Twentieth century agricultural drainage creates more erosive rivers. Hydrological Processes, 28, 1951-1961.

Strunk, H., 2003, Soil degradation and overland flow as causes of gully erosion on mountain pastures and in forests. Catena, 50, 185-198.

Thomas, A.W., Welch, R., Jordan, T.R., 1986, Quantifying concentrated-flow erosion on cropland with aerial photogrammetry. Journal of Soil and Water Conservation, 41, 249-252.

Twiddle, C.L., Bunting, M.J., 2010, Experimental investigations into the preservation of pollen grains: A pilot study of four pollen types. Review of Palaeobotany and Palynology, 162, 621-630.

Vanacker, V., Govers, G., Poesen, J., Deckers, J., Dercon, G., Loaiza, G., 2003, The impact of environmental change on the intensity and spatial pattern of water erosion in a semi-arid mountainous Andean environment. Catena, 51, 329-347.

Vanderkerckhove, L., Poesen, J., Govers, G., 2003, Medium-term gully headcut retreat rates in Southeast Spain determined from aerial photographs and ground measurements. Catena, 2003, 329-352.

White, S., 1996, Erosion, sediment delivery and sediment yield patterns in the Philippines. International Association of Hydrological Sciences, 236, 233-240.

Willard, D.A., Cronin, T.M., Verardo, S., 2003, Late-Holocene climate and ecosystem history from Chesapeake Bay sediment cores, USA. The Holocene, 13, 201-214.

Appendix 1: Field sampling procedures and lab sampling techniques

Before entering the field, I created a list of criteria that ravine alluvial fans must meet. With a one-meter lidar DEM and a shapefile of the delineated ravines, I selected by attributes ravines that deposited an alluvial fan on a terrace (Category 2 from Table 1) and were also bisected by a channel, which were separated out from all ravines with alluvial fans by visual inspection of the DEM. This led to a pool of 17 potential fans. Since 17 was too many ravines to sample in a six-week field season, selecting ravines that were easily accessible by road narrowed the sampling size down to six. These remaining ravines were of different geometries, incision depths, and location within the knickzone (Table 4).

Sampling in the field required a two-meter long hand auger, several boxes of sample zip bags, and detailed notes for record keeping. Grimley and Arruda (2007) and personal recommendations from David Grimley (Illinois State Geological Survey) suggested sampling in closer intervals for the first 40-centimeters of alluvial fan, then increasing spacing until the limit of the hand auger was reached. Sampling was conducted at 10-, 20-, 40-, 100-, and 200-centimeters. Sample depths were marked out with a measuring tape, and a sample was bagged once the auger reached the desired depth. All the samples were stored for analysis back at the lab.

All samples were air dried, crushed with a mortar and pestle, and sieved through a 180-μm sieve to filter out 20-grams of silt-sized particles. 20-grams from each bore hole was mixed with 10-mL of sodium-hexametaphosphate to break up silt cohesion and 250-mL of deionized water. With a magnetic stirrer, this mixture was blended for five minutes at low speed. Then the magnetic fraction that collected on the stirrer was rinsed off with deionized water into a separate 100-mL beaker, which was labeled with the site name and depth. If too little material attached to the stirrer, the mixture was blended for an additional two minutes and rinsed into the same 100-mL beaker. The 100-mL beakers with the separate magnetic fraction that contained fly ash were dried in an oven at 55 Celsius. Oftentimes, the dried fraction stuck to the bottom of the beaker. The dried magnetic fraction was gently loosened at the bottom of the beaker with a thin paintbrush. Then, another magnet inside a plastic bag was inserted into the beaker to attract loose magnetic particles, then carefully transferred over to a nearby one-inch by one-inch by one-half-inch clear plastic cube. With the corner of the plastic bag and magnetic fraction touching the inside of the cube, the magnet was quickly lifted out so the dried fraction fell into the cube for storage and analysis under the visual light microscope (Figure 22).

Figure 22. An example of an SEM mount (left) and visual light microscope storage cube (right).

Microscope analysis was done under a Zeiss transmitted and reflected light microscope and a JEOL scanning electron microscope. All cubes were placed under the Zeiss microscope at 250-x magnification for the presence-absence survey. I counted all fly ash grains from each sample depth, on one borehole site, at each alluvial fan for the modified light microscope survey. For the SEM survey, I took the top and bottom stratigraphic cube from one borehole and counted each fly ash grain on an SEM mount. Since there was ample magnetic fraction to fit on a carbon-taped SEM mount, I 3D-printed a small sediment splitter that evenly divided the dried magnetic fraction from one cube into six smaller fractions. Each SEM mount was given a thin carbon coating to prevent magnetic fraction mobility within the SEM vacuum and to increase conductivity for better image quality.

Appendix 2: Fly ash presence-absence survey

Sample	Depth (cm)	Fly Ash?	Sample	Depth (cm)	Fly Ash?
Mel 1	10	Yes	Magdalena 1	10	Yes
Mel 1	20	Yes	Magdalena 1	20	No
Mel 1	40	Yes	Magdalena 1	40	No
Mel 1	100	Yes	Magdalena 1	100	No
Mel 1	200	Yes	Magdalena 3	10	Yes
Mel 2	10	Yes	Magdalena 3	20	Yes
Mel 2	20	Yes	Magdalena 3	40	Yes
Mel 2	40	Yes	Magdalena 3	100	No
Mel 2	100	Yes	Magdalena 3	200	No
Mel 2	135	No	Magdalena 4	10	Yes
Mel 2	150	No	Magdalena 4	20	Yes
Mel 3	10	Yes	Magdalena 4	40	Yes
Mel 3	20	Yes	Magdalena 4	100	Yes
Mel 3	40	Yes	Magdalena 4	200	No
Mel 3	100	Yes	Magdalena 5	10	Yes
Mel 3	135	Yes	Magdalena 5	20	Yes
Mel 4	10	Yes	Magdalena 5	40	Yes
Mel 4	20	Yes	Magdalena 5	100	Yes
Mel 4	40	No	Magdalena 5	200	No
Mel 4	100	No	Magdalena 6	10	Yes
Mel 4	200	No	Magdalena 6	20	Yes
Mel 6	10	Yes	Magdalena 6	40	Yes
Mel 6	20	Yes	Magdalena 6	100	No
Mel 6	40	No	Magdalena 6	170	No
Mel 6	100	No	Magdalena 7	10	Yes
Mel 6	200	No	Magdalena 7	20	Yes
Mel 7	10	Yes	Magdalena 7	40	Yes
Mel 7	20	Yes	Magdalena 7	100	Yes
Mel 7	40	Yes	Magdalena 7	200	Yes
Mel 7	100	No	Magdalena 8	10	Yes
Mel 7	200	No	Magdalena 8	20	Yes
Mel 8	125	Yes	Magdalena 8	40	Yes
Mel 8	153	No	Magdalena 8	200	Yes
Mel 8	164	Yes	Magdalena 9	10	Yes
Mel 8	180	Yes	Magdalena 9	20	Yes
Mel 9	10	Yes	Magdalena 9	40	Yes
Mel 9	20	Yes	Magdalena 9	200	Yes
Mel 9	40	Yes			
Mel 9	100	Yes			

Sample	Depth (cm)	Fly Ash?	Sample	Depth (cm)	Fly Ash?
Catalina 3	10	Yes	Leigh 1	10	Yes
Catalina 3	20	Yes	Leigh 1	20	Yes
Catalina 3	40	Yes	Leigh 1	40	Yes
Catalina 3	100	Yes	Leigh 1	100	Yes
Catalina 3	200	Yes	Leigh 1	200	No
Catalina 4	10	Yes	Leigh 2	10	Yes
Catalina 4	20	Yes	Leigh 2	20	Yes
Catalina 4	40	Yes	Leigh 2	40	Yes
Catalina 4	100	Yes	Leigh 2	100	Yes
Catalina 4	200	No	Leigh 2	200	Yes
Catalina 5	10	Yes	Leigh 3	10	Yes
Catalina 5	20	Yes	Leigh 3	20	Yes
Catalina 5	55	No	Leigh 3	40	Yes
Catalina 5	100	No	Leigh 3	200	No
Catalina 6	10	Yes	Leigh 4	10	Yes
Catalina 6	20	Yes	Leigh 4	20	Yes
Catalina 6	40	Yes	Leigh 4	40	Yes
Catalina 6	100	Yes	Leigh 4	100	Yes
Catalina 6	200	No	Leigh 4	200	Yes
Catalina 7	10	Yes	Leigh 5	10	Yes
Catalina 7	20	Yes	Leigh 5	20	Yes
Catalina 7	40	Yes	Leigh 5	40	Yes
Catalina 7	100	Yes	Leigh 5	100	Yes
Catalina 7	175	Yes	Leigh 5	200	Yes
Catalina 7	200	No	Leigh 6	10	Yes
Catalina 8	10	Yes	Leigh 6	20	Yes
Catalina 8	20	Yes	Leigh 6	40	Yes
Catalina 8	40	Yes	Leigh 6	100	Yes
Catalina 8	100	Yes	Leigh 6	200	Yes
Catalina 8	200	Yes	Leigh 7	520	Yes
Catalina 9	10	Yes			
Catalina 9	20	Yes			
Catalina 9	40	Yes			
Catalina 9	100	Yes			
Catalina 9	200	Yes			

Sample	Depth (cm)	Fly Ash?	Sample	Depth (cm)	Fly Ash?
Lola 1	10	Yes	Lola 11	10	Yes
Lola 1	20	Yes	Lola 11	20	Yes
Lola 1	40	Yes	Lola 11	40	Yes
Lola 2	10	Yes	Lola 11	100	Yes
Lola 2	20	Yes	Lola 11	200	Yes
Lola 2	40	Yes	Loren 1	15	Yes
Lola 2	100	Yes	Loren 1	30	Yes
Lola 2	200	Yes	Loren 1	45	Yes
Lola 3	10	Yes	Loren 2	15	Yes
Lola 3	20	Yes	Loren 2	30	Yes
Lola 3	40	Yes	Loren 3	10	Yes
Lola 3	100	Yes	Loren 3	20	Yes
Lola 3	200	Yes	Loren 3	40	Yes
Lola 4	10	Yes	Loren 3	100	Yes
Lola 4	20	Yes	Loren 3	153	Yes
Lola 4	40	Yes	Loren 4	10	Yes
Lola 4	100	Yes	Loren 4	20	Yes
Lola 5	10	Yes	Loren 4	40	Yes
Lola 5	20	Yes	Loren 4	100	No
Lola 5	40	Yes	Loren 4	200	Yes
Lola 5	100	Yes	Loren 5	10	Yes
Lola 5	140	Yes	Loren 5	20	Yes
Lola 6	10	Yes	Loren 5	40	Yes
Lola 6	20	Yes	Loren 5	100	Yes
Lola 6	40	Yes	Loren 5	200	Yes
Lola 6	100	Yes	Loren 6	10	Yes
Lola 6	200	Yes	Loren 6	20	Yes
Lola 7	10	Yes	Loren 6	40	Yes
Lola 7	20	Yes	Loren 6	100	Yes
Lola 7	40	Yes	Loren 6	200	No
Lola 7	100	Yes	Loren 7	10	All Rocks
Lola 8	10	Yes	Loren 7	20	Yes
Lola 8	20	Yes	Loren 7	40	Yes
Lola 8	40	Yes	Loren 7	100	Yes
Lola 8	100	Yes	Loren 7	200	No
Lola 9	20	Yes	Loren 8	10	Yes
Lola 9	40	Yes	Loren 8	20	Yes
Lola 9	110	Yes			
Lola 10	10	Yes			
Lola 10	20	Yes			
Lola 10	40	Yes			
Lola 10	100	Yes			
Lola 10	200	Yes			

Appendix 3: Fly ash SEM counts

Sample	Depth (cm)	Count
Mel 1	10	23
Mel 8	180	1
Magdalena 7	10	14
Magdalena 7	200	4
Catalina 7	10	77
Catalina 7	200	23
Leigh 4	10	67
Leigh 4	200	21
Lola 2	10	11
Lola 2	200	6
Loren 4	10	63
Loren 4	200	10

Appendix 4: Fly ash modified light microscope survey

Sample	Depth	Count
Mel 3	10	21
Mel 3	20	9
Mel 3	40	7
Mel 3	100	10
Mel 3	135	8
Magdalena 5	10	12
Magdalena 5	20	2
Magdalena 5	40	3
Magdalena 5	100	1
Magdalena 5	200	1
Catalina 8	10	43
Catalina 8	20	21
Catalina 8	40	19
Catalina 8	100	11
Catalina 8	200	4
Leigh 6	10	56
Leigh 6	20	18
Leigh 6	40	3
Leigh 6	100	3
Leigh 6	200	7
Lola 3	10	33
Lola 3	20	16
Lola 3	40	5
Lola 3	100	8
Lola 3	200	3
Loren 5	10	41
Loren 5	20	33
Loren 5	40	19
Loren 5	100	0
Loren 5	200	2

Appendix 5: Fly ash weathering patterns

Sample	Depth (cm)	Count	Unweathered	Slightly Weathered	Weathered	Severely Weathered
Mel 10cm	10	23	18	2	3	0
Mel 180cm	180	1	0	0	1	0
Magdalena 10cm	10	14	8	5	1	0
Magdalena 200cm	200	4	0	2	2	0
Catalina 10cm	10	77	45	22	8	2
Catalina 200cm	200	23	6	8	9	0
Leigh 10cm	10	67	40	14	9	3
Leigh 200cm	200	21	9	9	2	1
Lola 10cm	10	11	7	2	1	1
Lola 200cm	200	6	1	3	1	1
Loren 10cm	10	63	37	14	4	7
Loren 200cm	200	10	0	1	6	3

Appendix 6: Fly ash EDS report example

3.17

1/26/2017 11:06:44 AM

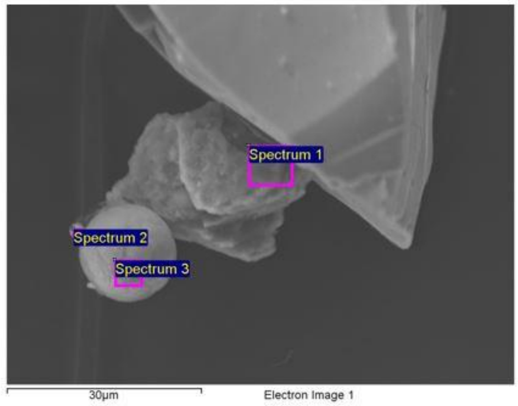

Electron Image 1

Processing option : All elements analysed (Normalised)

Spectrum	In stats.	C	O	Mg	Al	Si	K	Ca	Ti	Cr	Fe	Zn	Total	
Spectrum 2	Yes		42.22	0.31	7.87	8.04	0.25	0.36	0.39		39.57	0.99	100.00	
Spectrum 3	Yes		23.39		1.68	3.45			0.42		71.06		100.00	
Max.		6.66	42.22	0.31	7.87	8.04	0.25	0.36	0.81	0.27	89.38	0.99		
Min.		6.66	2.42	0.31	0.19	0.28	0.25	0.36	0.39	0.27	39.57	0.99		

All reports available in digital supplement.

Appendix 7: NRCS Charts and B-horizon depths

Blue Earth County, Minnesota

451—Dorchester loam, 1 to 3 percent slopes

Map Unit Setting

National map unit symbol: f98f
Elevation: 700 to 1,570 feet
Mean annual precipitation: 23 to 35 inches
Mean annual air temperature: 43 to 50 degrees F
Frost-free period: 155 to 200 days
Farmland classification: All areas are prime farmland

Map Unit Composition

Dorchester, rarely flooded, and similar soils: 90 percent
Minor components: 10 percent
Estimates are based on observations, descriptions, and transects of the mapunit.

Description of Dorchester, Rarely Flooded

Setting

Landform: Terraces
Landform position (two-dimensional): Backslope
Down-slope shape: Linear
Across-slope shape: Linear
Parent material: Loamy alluvium

Typical profile

Ap - 0 to 10 inches: loam
C - 10 to 46 inches: stratified loamy fine sand to loam to silt loam
Ab - 46 to 60 inches: loam

Properties and qualities

Slope: 1 to 3 percent
Depth to restrictive feature: More than 80 inches
Natural drainage class: Moderately well drained
Capacity of the most limiting layer to transmit water (Ksat): Moderately high to high (0.57 to 1.98 in/hr)
Depth to water table: About 30 to 43 inches
Frequency of flooding: Rare
Frequency of ponding: None
Calcium carbonate, maximum in profile: 30 percent
Available water storage in profile: Very high (about 12.8 inches)

Interpretive groups

Land capability classification (irrigated): None specified
Land capability classification (nonirrigated): 2w
Hydrologic Soil Group: C
Ecological site: Loamy Floodplains (F103XY032MN)
Other vegetative classification: Sloping Upland, Calcareous (G103XS010MN)
Hydric soil rating: No

Blue Earth County, Minnesota

1002—Alluvial land, frequently flooded

Map Unit Setting

National map unit symbol: f95v
Elevation: 700 to 1,570 feet
Mean annual precipitation: 23 to 35 inches
Mean annual air temperature: 43 to 50 degrees F
Frost-free period: 155 to 200 days
Farmland classification: Not prime farmland

Map Unit Composition

Alluvial land, frequently flooded, and similar soils: 90 percent
Minor components: 10 percent
Estimates are based on observations, descriptions, and transects of the mapunit.

Description of Alluvial Land, Frequently Flooded

Setting

Landform: Flood plains
Down-slope shape: Linear
Across-slope shape: Concave
Parent material: Fine-loamy alluvium

Typical profile

A1 - 0 to 12 inches: silty clay loam
A2 - 12 to 30 inches: loam
A3 - 30 to 55 inches: stratified fine sandy loam to loam
AB,Bg - 55 to 80 inches: fine sandy loam

Properties and qualities

Slope: 0 to 2 percent
Depth to restrictive feature: More than 80 inches
Natural drainage class: Poorly drained
Capacity of the most limiting layer to transmit water (Ksat): Moderately high to high (0.57 to 1.98 in/hr)
Depth to water table: About 6 to 18 inches
Frequency of flooding: Frequent
Frequency of ponding: None
Calcium carbonate, maximum in profile: 20 percent
Available water storage in profile: Very high (about 12.3 inches)

Interpretive groups

Land capability classification (irrigated): None specified
Land capability classification (nonirrigated): 5w
Hydrologic Soil Group: B/D
Ecological site: Wet Floodplains (F103XY033MN)
Other vegetative classification: Frequently Flooded (G103XS016MN)
Hydric soil rating: Yes

Blue Earth County, Minnesota

94C—Terril loam, 6 to 15 percent slopes

Map Unit Setting

National map unit symbol: f99k
Elevation: 700 to 1,570 feet
Mean annual precipitation: 23 to 35 inches
Mean annual air temperature: 43 to 50 degrees F
Frost-free period: 155 to 200 days
Farmland classification: Farmland of statewide importance

Map Unit Composition

Terril and similar soils: 90 percent
Minor components: 10 percent
Estimates are based on observations, descriptions, and transects of the mapunit.

Description of Terril

Setting

Landform: Hills on moraines
Landform position (two-dimensional): Footslope
Down-slope shape: Concave
Across-slope shape: Linear
Parent material: Fine-loamy colluvium

Typical profile

Ap,A - 0 to 21 inches: loam
Bw - 21 to 49 inches: loam
C - 49 to 60 inches: loam

Properties and qualities

Slope: 6 to 15 percent
Depth to restrictive feature: More than 80 inches
Natural drainage class: Moderately well drained
Capacity of the most limiting layer to transmit water (Ksat): Moderately high to high (0.57 to 1.98 in/hr)
Depth to water table: More than 80 inches
Frequency of flooding: None
Frequency of ponding: None
Calcium carbonate, maximum in profile: 15 percent
Available water storage in profile: High (about 11.3 inches)

Interpretive groups

Land capability classification (irrigated): None specified
Land capability classification (nonirrigated): 3e
Hydrologic Soil Group: B
Ecological site: Footslope/Drainageway Prairies (R103XY011MN)
Other vegetative classification: Sloping Upland, Neutral (G103XS002MN)
Hydric soil rating: No

Blue Earth County, Minnesota

451—Dorchester loam, 1 to 3 percent slopes

Map Unit Setting

National map unit symbol: f98f
Elevation: 700 to 1,570 feet
Mean annual precipitation: 23 to 35 inches
Mean annual air temperature: 43 to 50 degrees F
Frost-free period: 155 to 200 days
Farmland classification: All areas are prime farmland

Map Unit Composition

Dorchester, rarely flooded, and similar soils: 90 percent
Minor components: 10 percent
Estimates are based on observations, descriptions, and transects of the mapunit.

Description of Dorchester, Rarely Flooded

Setting

Landform: Terraces
Landform position (two-dimensional): Backslope
Down-slope shape: Linear
Across-slope shape: Linear
Parent material: Loamy alluvium

Typical profile

Ap - 0 to 10 inches: loam
C - 10 to 46 inches: stratified loamy fine sand to loam to silt loam
Ab - 46 to 60 inches: loam

Properties and qualities

Slope: 1 to 3 percent
Depth to restrictive feature: More than 80 inches
Natural drainage class: Moderately well drained
Capacity of the most limiting layer to transmit water (Ksat): Moderately high to high (0.57 to 1.98 in/hr)
Depth to water table: About 30 to 43 inches
Frequency of flooding: Rare
Frequency of ponding: None
Calcium carbonate, maximum in profile: 30 percent
Available water storage in profile: Very high (about 12.8 inches)

Interpretive groups

Land capability classification (irrigated): None specified
Land capability classification (nonirrigated): 2w
Hydrologic Soil Group: C
Ecological site: Loamy Floodplains (F103XY032MN)
Other vegetative classification: Sloping Upland, Calcareous (G103XS010MN)
Hydric soil rating: No

Blue Earth County, Minnesota

94B—Terril loam, 2 to 6 percent slopes

Map Unit Setting

National map unit symbol: 2tsjq
Elevation: 690 to 1,840 feet
Mean annual precipitation: 24 to 37 inches
Mean annual air temperature: 43 to 52 degrees F
Frost-free period: 140 to 180 days
Farmland classification: All areas are prime farmland

Map Unit Composition

Terril and similar soils: 80 percent
Minor components: 20 percent
Estimates are based on observations, descriptions, and transects of the mapunit.

Description of Terril

Setting

Landform: Ground moraines
Landform position (two-dimensional): Footslope, toeslope
Landform position (three-dimensional): Dip
Down-slope shape: Concave
Across-slope shape: Linear
Parent material: Colluvium

Typical profile

Ap - 0 to 9 inches: loam
A - 9 to 34 inches: loam
Bw - 34 to 52 inches: loam
C - 52 to 79 inches: loam

Properties and qualities

Slope: 2 to 6 percent
Depth to restrictive feature: More than 80 inches
Natural drainage class: Well drained
Capacity of the most limiting layer to transmit water (Ksat): Moderately high to high (0.20 to 2.00 in/hr)
Depth to water table: About 39 to 51 inches
Frequency of flooding: None
Frequency of ponding: None
Calcium carbonate, maximum in profile: 20 percent
Salinity, maximum in profile: Nonsaline to very slightly saline (0.0 to 2.0 mmhos/cm)
Available water storage in profile: High (about 11.0 inches)

Interpretive groups

Land capability classification (irrigated): None specified
Land capability classification (nonirrigated): 2e
Hydrologic Soil Group: B

Fom
Lola terrace.

Blue Earth County, Minnesota

17—Minneopa sandy loam, 0 to 3 percent slopes

Map Unit Setting

National map unit symbol: f96v
Elevation: 700 to 1,570 feet
Mean annual precipitation: 23 to 35 inches
Mean annual air temperature: 43 to 50 degrees F
Frost-free period: 155 to 200 days
Farmland classification: Farmland of statewide importance

Map Unit Composition

Minneopa and similar soils: 90 percent
Minor components: 10 percent
Estimates are based on observations, descriptions, and transects of the mapunit.

Description of Minneopa

Setting

Landform: Terraces
Down-slope shape: Linear
Across-slope shape: Linear
Parent material: Coarse-loamy outwash over sandy outwash

Typical profile

Ap,A - 0 to 15 inches: sandy loam
Bw - 15 to 20 inches: sandy loam
2C - 20 to 60 inches: loamy sand

Properties and qualities

Slope: 0 to 3 percent
Depth to restrictive feature: More than 80 inches
Natural drainage class: Moderately well drained
Capacity of the most limiting layer to transmit water (Ksat): High (1.98 to 5.95 in/hr)
Depth to water table: About 43 to 60 inches
Frequency of flooding: None
Frequency of ponding: None
Calcium carbonate, maximum in profile: 15 percent
Available water storage in profile: Low (about 5.3 inches)

Interpretive groups

Land capability classification (irrigated): None specified
Land capability classification (nonirrigated): 3s
Hydrologic Soil Group: A
Ecological site: Sandy Upland Prairies (R103XY003MN)
Other vegetative classification: Sloping Upland, Low AWC, Acid (G103XS008MN)
Hydric soil rating: No

Loren Lavine

Blue Earth County, Minnesota

961—Storden complex, very steep

Map Unit Setting

National map unit symbol: f99n
Elevation: 700 to 1,570 feet
Mean annual precipitation: 23 to 35 inches
Mean annual air temperature: 43 to 50 degrees F
Frost-free period: 155 to 200 days
Farmland classification: Not prime farmland

Map Unit Composition

Storden and similar soils: 70 percent
Lester and similar soils: 25 percent
Minor components: 5 percent
Estimates are based on observations, descriptions, and transects of the mapunit.

Description of Storden

Setting

Landform: Hills on moraines
Landform position (two-dimensional): Shoulder
Down-slope shape: Convex
Across-slope shape: Convex
Parent material: Fine-loamy till

Typical profile

A - 0 to 8 inches: loam
C - 8 to 60 inches: loam

Properties and qualities

Slope: 45 to 65 percent
Depth to restrictive feature: More than 80 inches
Natural drainage class: Well drained
Capacity of the most limiting layer to transmit water (Ksat): Moderately high to high (0.57 to 1.98 in/hr)
Depth to water table: More than 80 inches
Frequency of flooding: None
Frequency of ponding: None
Calcium carbonate, maximum in profile: 30 percent
Available water storage in profile: High (about 10.5 inches)

Interpretive groups

Land capability classification (irrigated): None specified
Land capability classification (nonirrigated): 7e
Hydrologic Soil Group: B
Ecological site: Calcareous Upland Prairies (R103XY002MN)
Other vegetative classification: Not Suited (G103XS024MN)
Hydric soil rating: No